Liquid Crystals
Publication details, including instructions for authors and subscription information:
http://www.informaworld.com/smpp/title~content=t713926090

Optic mode determination of the relaxed state configuration in a ferroelectric liquid crystal cell

S. J. Elston[a]
[a] Thin Film and Interface Group, Department of Physics, University of Exeter, Exeter, England

To cite this Article Elston, S. J.(1991) 'Optic mode determination of the relaxed state configuration in a ferroelectric liquid crystal cell', Liquid Crystals, 9: 6, 769 — 806
To link to this Article: DOI: 10.1080/02678299108055002
URL: http://dx.doi.org/10.1080/02678299108055002

LIQUID CRYSTALS, 1991, VOL. 9, NO. 6, 769–806

Optic mode determination of the relaxed state configuration in a ferroelectric liquid crystal cell

by S. J. ELSTON

Thin Film and Interface Group, Department of Physics,
University of Exeter, Stocker Road, Exeter EX4 4QL, England

(*Received 2 October 1990; accepted 27 December 1990*)

Here the method of propagation of optic modes to examine the alignment in a ferroelectric liquid crystal layer is fully discussed. A sample geometry which allows the excitation of optic modes in a ferroelectric liquid crystal cell is presented and the data obtained in terms of reflectivity. The data are analysed by modelling the expected reflectivity from such a cell for a selection of proposed models for the optic tensor configuration. Models where the smectic layering lies perpendicular to the cell surfaces, or bends slowly across a cell are seen to be incorrect. It is found that a discontinuity in the smectic layering in the middle of the cell must be included to model the data well. This is consistent with the chevron structure seen in X-ray scattering work, and leads to an optic tensor alignment which is largely uniform across the ferroelectric layer. The relation between this and observation of conventional ferroelectric cells is discussed.

1. Introduction

In his founding work on chiral smectic C ferroelectric liquid crystals Meyer predicted in 1975 that it would be possible to produce a cell containing this material which would exhibit bi-stable properties [1]. A device of this nature, using surface stabilization to retain two switched states was engineered in 1980 by Clark and Lagerwall [2]. In this device the ferroelectric properties of the S_C^* liquid crystal were used to allow the switching by application of DC pulses across a cell between two states of differing optic tensor orientation. Observation of such a cell between crossed polaroids shows two stable optic tensor positions, aligning the axis of one of these along one of the polarizer axes allows a device to be built which switches between a transmission and extinction state (both of which are stable). This opened up the possibility of building large ferroelectric liquid crystal display panels [2].

Work performed in the past on the examination of the precise alignment in such ferroelectric devices has concentrated on the use of polarized optical microscopy as a method to examine the optical dielectric tensor configuration [3]. Examination of such a cell in a polarizing microscope reveals various coloured states, and these can be interpreted in terms of director configurations within the cell. For a number of years it was believed that the smectic layering in the cells lay perpendicular to the cell walls in the bookshelf geometry, and results were interpreted in terms of optic tensor configurations within this structure [2]. However work using X-ray scattering techniques reveals that the smectic layering is in fact not normal to the cell surfaces, but is tilted in a chevron structure [4, 5]. The formation of this structure is due to the molecular rearrangement within the smectic layering between the smectic A and S_C^* phases which results in a layer shrinkage and consequent layer tilt in order to retain continuity in the cell. This chevron structure leads to the re-interpretation of polarized

0267–8292/91 $3·00

microscopy data in terms of optic tensor configurations consistent with this form in the smectic layering [5]. However the difficulties in putting a precise interpretation on the optical results indicates the need for further work.

Here the optic tensor configuration in a thin layer of ferroelectric liquid crystal material is investigated in an alternative way. By coupling to optic modes which can be supported by such a layer it is possible to determine more fully the optic tensor configuration. This technique has been used previously to study the optical properties, and hence director configuration in a thin layer of nematic liquid crystal [6]. In a previous letter we have shown that this technique applied to ferroelectric liquid crystal cells indicates that the configuration in the cell is largely equivalent to a uniform slab of material with the optic axis rotated from the surface alignment direction by a few degrees [7]. Here we explain more fully the methods used and the nature of the data taken. We also present a complete analysis of the data, and show the failure of several models previously proposed to explain the optic tensor configuration present in a cell. The result that the optic tensor is largely uniform is consistent with the X-ray data which indicated the chevron structure in the smectic layering. This provides, therefore, a direct optical confirmation of the structure.

2. Guided modes and surface plasmon polaritons

In a multi-layered medium various optic modes can be excited and propagated the general situation for this is well documented in the literature [8, 9]. For example, in a low/high/low refractive index layered system it is possible to propagate guided modes within the high refractive index layer due to total internal reflection at the layer interfaces. It is by the excitation and observation of optic modes supported in a thin layer of liquid crystal material that the structure in a ferroelectric liquid crystal filled cell is to be investigated here.

The system under consideration is shown in figure 1. Here light incident in the glass pyramids can couple evanescently through the thin silver film to excite optic modes

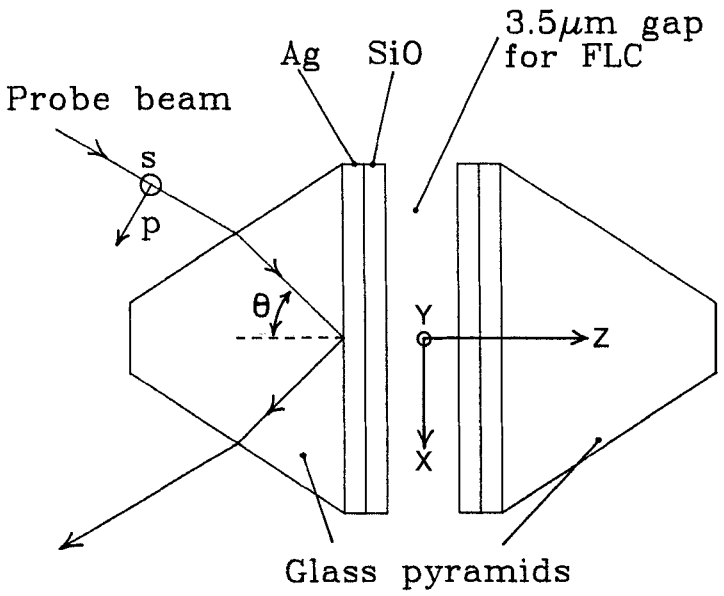

Figure 1. The sample cell construction used in the experimental work here.

which may be supported in the liquid crystal layer [10]. (Axes are set up as shown.) Then the indicant light and hence any modes which are excited propagate in the xz plane. The x direction is parallel to the cell surfaces, directed along the cell in the direction of mode propagation. Optic modes excited in the liquid crystal layer will propagate purely in the positive x direction. The z direction is perpendicular to the cell surfaces. The positive z direction is away from the front face of the cell, in the direction of the component of incident light which is perpendicular to the cell surfaces. Then the y direction is perpendicular to these, that is transverse to the plane of incidence (or propagation) of the light. The positive y direction is set to give a right handed set of axes xyz. Within this system of axes there are two orientations of the liquid crystal cell which are of interest and used in the work here. If the surface alignment direction of the cell lies in the xz plane this is termed the parallel orientation. This is when the nematic phase in a homogeneous aligned cell has the director (and hence major optic axis) in the plane of light propagation. This is termed the parallel orientation of the cell because the surface alignment direction (direction of the nematic director at the cell surfaces) is parallel to the plane in which the light propagates. Alternatively the cell can be rotated by 90° about the z axis to give the orthogonal orientation. Then the nematic surface alignment direction lies in the y direction. This is termed the perpendicular orientation. This system of axes for light propagation in the sample and terms for the two cell orientations are to be used throughout this paper.

Light incident in one of the glass pyramids in general reflects from the silver film. There is, however, an evanescently decaying field within the film. If the silver film is chosen to be of the correct thickness the optic field penetrates through the film and can excite modes in the liquid crystal layer. The momentum coupling condition is

$$k_{\text{mode}} = k_{xx} = nk \sin\theta = \frac{\omega}{c}\sqrt{\varepsilon_g}\sin\theta,$$

where k_{mode} is the wavevector of a supported mode along the liquid crystal layer, in the x direction, k_{xx} is the wavevector in the x direction, this is always conserved, and n is the refractive index of the pyramid. Here work is done at a constant wavelength of 632·8 nm (He–Ne laser source) for which n is always 1·8 for the high index glass from which the pyramids forming the cell are made. This is equivalent to a dielectric constant of the glass, $\varepsilon_g = 3{\cdot}24$, assuming that it is purely real (i.e. there is no absorption in the glass). k is the wavevector of the incident photon in free space; this is equivalent to the angular frequency divided by the speed of light (ω/c) for the incident light in air, assuming that the air has refractive index of 1·0 (actually 1·0003 at 632·8 nm).

Finally θ is the angle of incidence of the light to the cell surface (xy plane) within the glass pyramid. Hence modes of various momenta can be excited by varying the angle of incidence θ.

When the coupling condition is satisfied and an optic mode is excited this is observed as a dip in the reflected intensity of the light. The reflectivity against angle of incidence curve thus obtained can be modelled theoretically [11] and hence, in principle, information about the layer in which the modes are propagating obtained. We now consider some of the optic modes which can be supported in this system. For simplicity the SiO layers shown in figure 1, which are present to align the liquid crystal in the cell, will be neglected for the purpose of describing the various optic modes which can be excited and observed. The system then used for the description of the supported modes is glass/silver/gap/silver/glass, where the gap can be filled with the liquid crystal material. The absence of the SiO in the modelling does not affect qualitatively the form

of the reflectivity. The presence of the SiO layers can be allowed for in the modelling of the full system, and the effect of their presence will be discussed later.

First consider the case when the gap in the cell contains an isotropic fluid. In this case it is immediately clear that the two possible orientations of the cell (parallel and perpendicular) are optically degenerate. Due to the high reflectivity of the silver layers this system can support resonant guided modes. These are not true waveguide modes but are Fabry–Perot type modes which propagate in the x direction in the isotropic layer. These resonant modes can be of two types, either transverse electric (TE) or transverse magnetic (TM). The former (TE) propagate with the electric field oriented perpendicular to the plane of propagation (i.e. E field in the y direction) and are excited

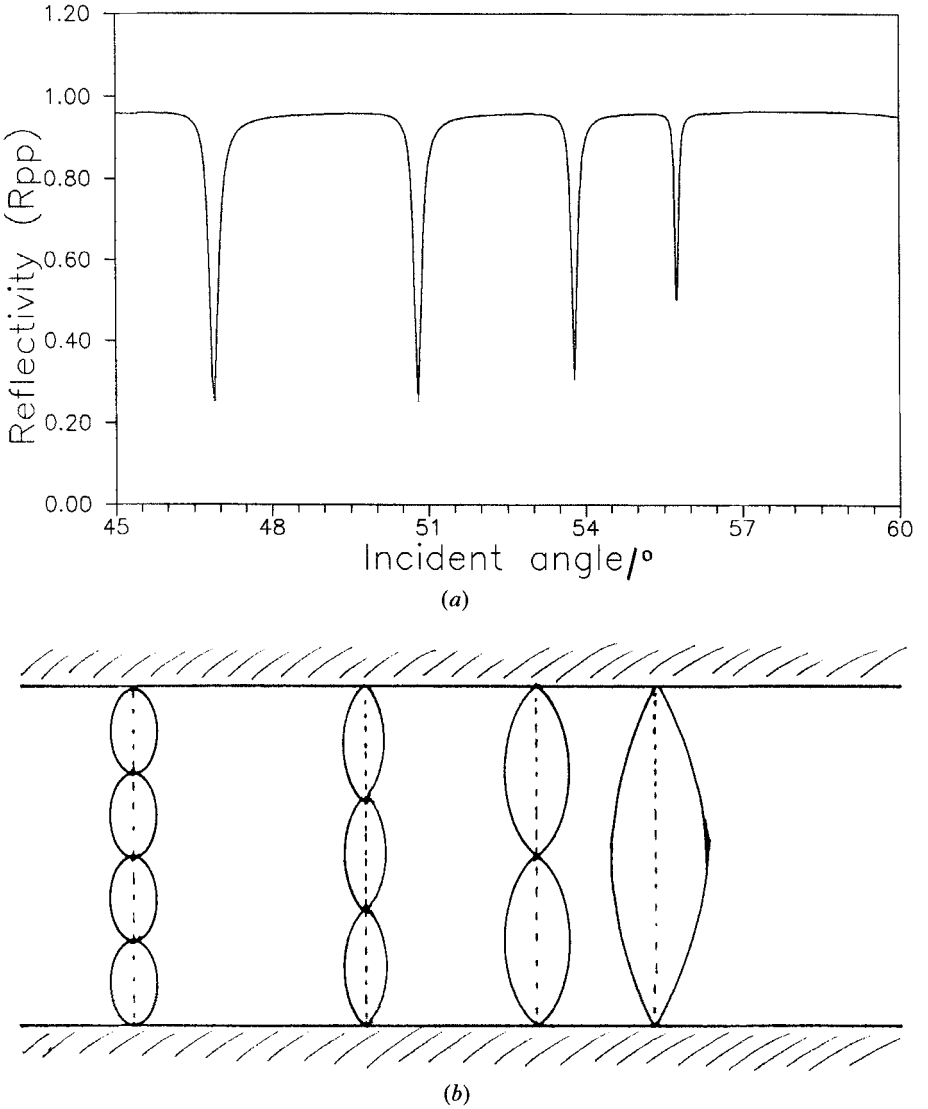

Figure 2. (*a*) Example plot of a reflectivity curve for p-polarized light for a sample filled with isotropic fluid. The series of sharp dips correspond to the excitation of guided modes in the cell. (*b*) The form of the E field distributions within the sample is illustrated.

with TE polarized light. This is, by convention, referred to as s-polarized light, and so TE modes can be referred to as s-modes. Alternatively TM modes propagate with the magnetic field oriented perpendicular to the plane of propagation (y direction), then the E field is in the xz plane. Such modes are excited with TM light, referred to as p-polarized light. Hence these modes are also referred to as p-modes.

An example of the reflectivity against angle of incidence curve for p-polarized light (termed R_{pp}) is shown in figure 2 (*a*). The reflectivity is near to unity for most of the data due to the high reflectivity of the silver layers. A series of sharp dips in the reflectivity are due to the excitation of p-modes (TM modes) in the isotropic layer. In this case positioning of these modes in θ depends mainly on two things, (*a*) the refractive index n of the fluid and (*b*) the cell thickness t. For increasing n the modes move to higher θ, that is their momentum increases. In particular it is noted that the guided modes are excited at angles below the critical angle between the glass and the layer of material in the gap,

$$\theta_{\text{modes}} < \sin^{-1}(n/n_{\text{glass}}).$$

The light tunnels through the silver barrier evanescently and couples directly to these modes in the gap. Modes may be excited at various angles between this critical angle and the angle $\theta = 0$ when the wavevector in the x direction (k_{xx}) becomes zero. For increasing cell thickness the modes become closer together, that is become separated less in momentum space. In the case illustrated here the index of the fluid is 1·5 and the cell thickness is 2·0 μm. It is seen that the modes are not delta functions, but have some spread in angle and hence in momentum, also. This is due to some absorption in the isotropic layer, and also because the cell is not a perfect guiding cavity. The silver films are not perfect reflectors, and therefore the resonances are not perfectly defined. (In the same way the finesse of a Fabry–Perot cavity defines the width of the peaks observed.) The dielectric constant at optic frequencies for the layer of material in the gap is written as

$$\varepsilon = \varepsilon' + i\varepsilon''.$$

Here ε' is the real part of the dielectric constant and is very nearly equal to n^2 for materials with low absorption (such as aligned liquid crystal) and ε'' is the imaginary part and represents the absorption in the system. In the example this is

$$\varepsilon = 2{\cdot}25 + 0{\cdot}001i.$$

This small absorption adds to the spread in angle over which a particular mode is excited. An increase in ε'' causes the width over which a mode is excited to increase, making the dips in the R_{pp} (and R_{ss}) curve broader and shallower.

Referring to figure 2 (*a*) the mode at highest θ is the lowest order mode. This has one E field peak across the layer as illustrated in figure 2 (*b*) and it is referred to as the TM_1 mode. The next mode is TM_2, and so on, as illustrated. The importance of the form of the E field across the layer will become apparent later on. Now by fitting theoretically calculated reflectivity curves to the reflectivity against angle of incidence data obtained in practice for isotropic layers, it is possible to determine the optic dielectric constant of the material and the cell thickness.

In this system it is also possible to excite and propagate surface plasmon-polaritons [12]. These are charge density electromagnetic field coupled oscillations which can be supported at an interface between media of opposite sign of real part of dielectric constant such that:

$$\varepsilon_1' + \varepsilon_2' < 0.$$

At 632·8 nm the dielectric constant of silver is

$$\varepsilon \approx -17+0{\cdot}7i,$$

hence the silver/fluid interface can support surface plasmon-polaritons. This is highly localized to the interface with exponentially decaying fields in each medium. Since it supports a charge density oscillation at the interface it is a TM mode (it can be referred to as the TM_0 mode) and for isotronic media is excited with p-polarized light only. s-polarized (TE) light has an E field component in the y direction only, and therefore none across the interface. The wavevector of the surface plasmon-polariton for the interface between two semi infinite media is given by [12]

$$k_{spp}=\frac{\omega}{c}\left(\frac{\varepsilon_1'\varepsilon_2'}{\varepsilon_1'+\varepsilon_2'}\right)^{1/2}.$$

Using this as an approximation for the system here and inserting

$\varepsilon_1' = -17$ for the silver,
$\varepsilon_2' = 2{\cdot}25$ for the liquid crystal layer,

then comparing with the earlier formula for k_{xx} the surface plasmon-polariton is expected to be excited at an angle of incidence, $\theta_{spp} \sim 65°$. The critical angle between media of dielectric constants 3·24 (the glass) and 2·25 (the fluid) is $\sim 56°$. It is seen, therefore, that the surface plasmon-polariton is excited above the critical angle between the glass and the fluid, and can therefore only be coupled to evanescently, since there is no propagating wave beyond the the front face of the pyramid (in the fluid) for light incident at angles above the critical angle. For the same system as the resonant guided modes shown previously the surface plasmon-polariton resonance is shown in figure 3, where the angle of incidence range extends above that in figure 2. This figure also illustrates the z component of the E field distribution within the system, showing that this is a surface mode with evanescently decaying field amplitudes into the silver and liquid crystal. Notice the reversal in the sign of E_z at the silver/liquid crystal interface, due to the opposite signs of the real part of the dielectric constants in the two materials.

Clearly the surface plasmon-polariton resonance is much broader in angle (and momentum) than the guided mode resonances. This is due to the high absorption of the silver layer ($\varepsilon'' \simeq 0{\cdot}7$) on which it propagates. Now the field from the surface plasmon-polariton decays exponentially into the fluid (as illustrated in the field plot of figure 3), within about 1/4 μm of the silver surface. Its excitation is, therefore, not dependent on the thickness of the cell, which is always greater than this. The surface localised properties of the surface plasmon-polariton resonance will later be seen to be an important property in the characterisation of the silver and SiO layers, and also allows coupling into interesting modes in the liquid crystal layer [13].

Now consider a slightly more complicated situation, with the cell gap being filled with a uniform uniaxial slab of dielectric material. This could be a homogeneously aligned liquid crystal in the nematic or smectic A phase, which are both optically equivalent to a uniaxial slab. The optic axis of the slab of material would lie parallel to the surface alignment direction throughout the cell. Now in this situation the two possible orientations of the cell (parallel and perpendicular) are no longer degenerate. The response will be different depending on whether the optic axis is aligned in the y direction (perpendicular to the plane of light propagation) or lies in the xz plane (parallel to the plane of propagation).

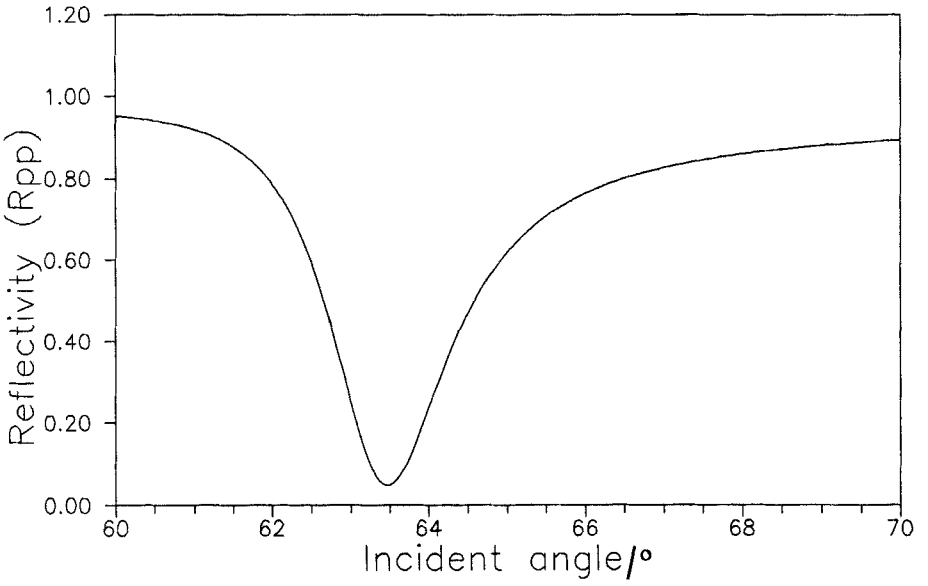

(*a*)

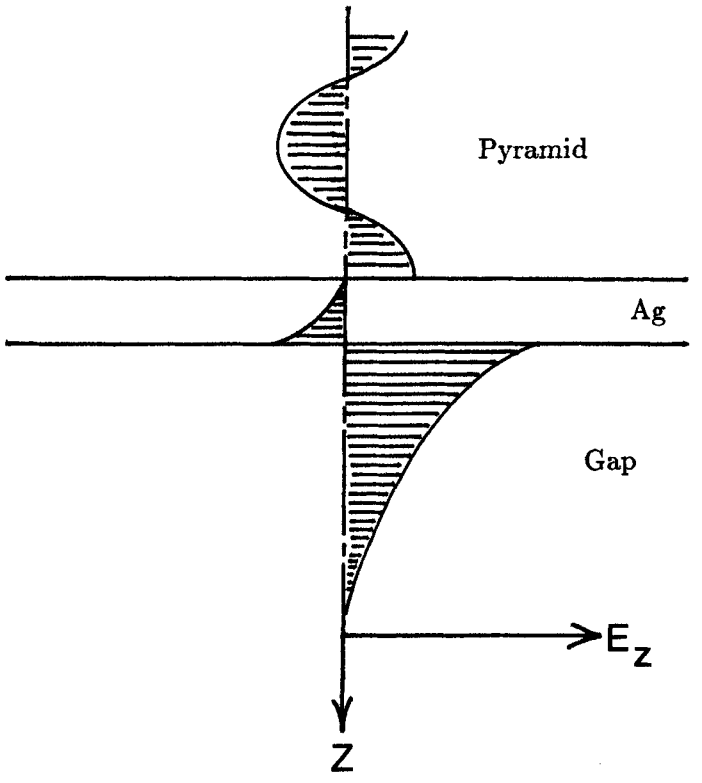

(*b*)

Figure 3. (*a*) The surface plasmon-polariton resonance reflectivity curve for p-polarized light. (*b*) Illustration of the distribution of the z component of electric field (E_z) through the system at the minimum.

When the optic axis is perpendicular to the xz plane s-polarized (TE) light will see $\varepsilon_{\parallel}$, that is the optical dielectric constant parallel to the optic axis. For material with low absorption this will be nearly equal to the square of the extraordinary refractive index, n_e^2. Hence the angles at which s-modes are excited depends now on $\varepsilon_{\parallel}$ and cell thickness. However p-polarized (TM) modes will see only $\varepsilon_{\perp}$, that is the optical dielectric constant perpendicular to the optic axis (equivalent to n_O^2). Hence the angles at which p-modes and the surface plasmon-polariton are excited depends on $\varepsilon_{\perp}$ and the cell thickness. So excitation of these modes should lead by comparison with theory to the determination of all the optic parameters of a layer of uniaxial material.

Alternatively if the cell is oriented with the optic axis parallel to the xz plane things are a little more difficult [14]. Now s-modes (TE) see $\varepsilon_{\perp}$ only, the angles at which they are excited then depend only on this and the cell thickness. However the angles at which p-modes (TM) are excited will depend on both $\varepsilon_{\perp}$ and $\varepsilon_{\parallel}$ (and, of course, cell thickness). The electric field of the p-modes within the uniaxial layer is oriented mainly in the z direction, so there is a strong dependence on $\varepsilon_{\perp}$. There is also some component of the E field in the x direction (i.e. the direction in which the mode propagates) and so there is a weak dependence on $\varepsilon_{\parallel}$. This can best be understood if the zig-zag ray picture for the mode propagating in the uniaxial layer is considered. Then, for any mode where the ray makes an angle with the optic axis which is not equal to zero there will be a dependence on $\varepsilon_{\parallel}$. This effect also occurs for the surface plasmon-polariton resonance, the momentum of which (and hence the angle of excitation) will depend strongly on $\varepsilon_{\perp}$ and weakly on $\varepsilon_{\parallel}$.

In general the layer in the gap may have an alignment which varies as a function of z. This could be a S_C^* liquid crystal which furthermore may be biaxial and which may not be a simple uniform slab aligned in the nematic surface alignment direction. In this case the optic modes which may be excited are considerably more complicated [15]. In particular if the axes of the optic tensor do not lie either in or perpendicular to the xz plane then the modes which are excited can be of mixed polarization. That is they are no longer either purely p-polarized (TM) or s-polarized (TE) modes but may become elliptically polarized s-p mixed modes. In general, modes become of mixed polarization if the optic tensor cannot be diagonalized in a set of orthogonal axes consisting of the y axis and a pair of axes in the xz plane. Off-diagonal terms in the optic dielectric tensor then couple between electric field components in the y direction and the xz plane and cause s–p mixing and mixed polarization modes. The excitation of such modes can lead to important information about the optic tensor orientation within the liquid crystal layer. Also the reflectivity as a function of incident angle becomes considerably more complicated, incident p- or s-polarized light can excite modes which are p-like or s-like respectively, but it is also possible for incident p-polarized light to excite s-like modes and vice versa.

In order to discuss the general situation it is necessary to set up the optic dielectric tensor of the material, and the angles which define its configuration within the cell. This is illustrated in figure 4 which shows the initial optic tensor orientation and the convention for the twist and tilt angles used to describe its configuration. Twist and tilt are defined in the following way. Twist is rotation of the tensor axes about an axis perpendicular to the cell surfaces, that is the z axis; this is equivalant to the first eulerian angle. This twists the optic tensor major axis out of the surface alignment direction within the layer of material. After a twist angle of a few degrees the optic tensor still lies orthogonalised in the plane of the cell surfaces, but with the major axis no longer in the surface alignment direction. Tilt is rotation of the tensor axes about an axis lying in the

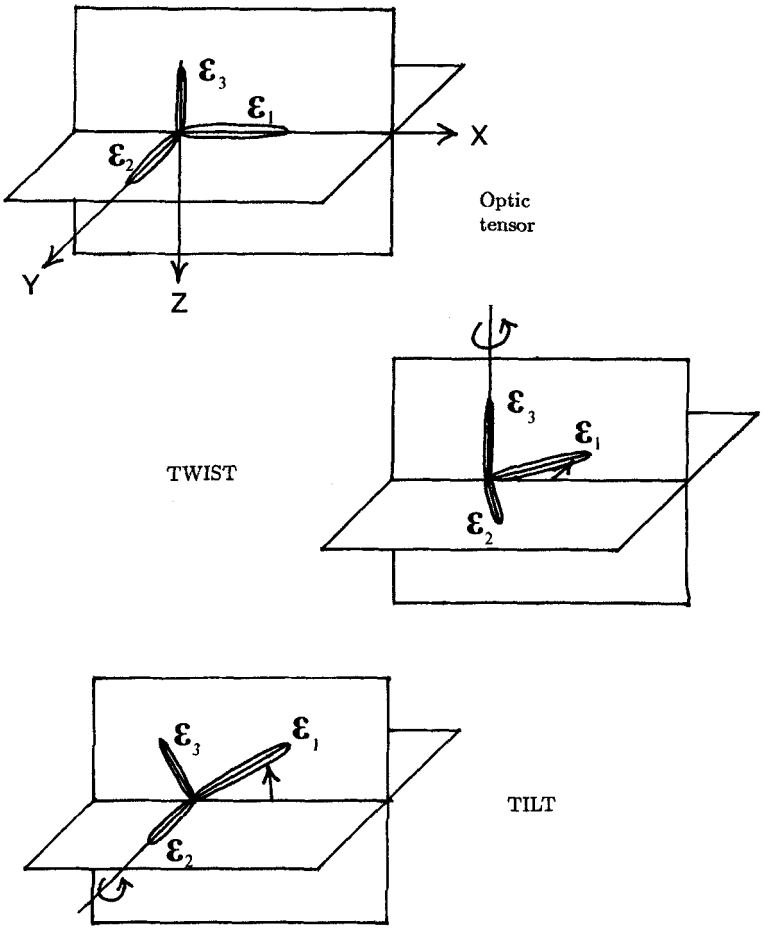

Figure 4. Definition of the Euler angles twist and tilt used to describe the optic tensor orientation in the cell.

plane of the cell surfaces (the xy plane) and perpendicular to the major axis of the optic tensor after it has travelled through the twist angle. This is equivalent to the second eulerian angle. After a tilt the optic tensor is not orthogonalized in the plane of the cell surfaces and the major axis no longer lies in the plane of the surfaces.

There are many (infinitely many!) possible situations in the general case, but to illustrate what may be observed in the reflectivity data some simple situations will be considered.

First consider the simple case of a tilted uniaxial layer. This is the same as the previous situation considered, but with the optic axis tilted a few degrees out of the plane of the cell surfaces. (This could be a tilted nematic layer). Now with this system in the parallel orientation $\varepsilon_{\|}$ lies in the xz plane. This then gives no s–p mixing since there is no component of the optic tensor which does not lie either in or orthogonal to the xz plane. The modes which may be excited are either purely s-polarized (seeing $\varepsilon_{\perp}$) or purely p-polarized (seeing some combination of $\varepsilon_{\perp}$ and $\varepsilon_{\|}$). However, with the cell in the perpendicular orientation the modes which can be excited are more interesting. In this case $\varepsilon_{\|}$ is tilted at an angle to the y axis. Now, therefore, the optic tensor axes lie such

that they are not orthogonalized in the y axis, xz plane system. This case then leads to the possibility of s–p mixing. To illustrate this the reflectivity for such a system as a function of angle of incidence for p-polarized light is shown in figure 5. This is clearly more complicated than forms considered thus far. First the broad surface plasmon-polariton resonance and the series of dips where p-like modes are excited are still seen. These are no longer purely p-modes though, but are elliptical modes with the main component of electric field still in the z direction. In addition to these modes there are also several weaker dips in the reflectivity and a series of sharp dips in the surface plasmon-polariton resonance itself. If the curve is compared with that for s-polarized light it is seen that these additional modes are excited at angles corresponding to the excitation of s-like modes. The explanation is that p-polarized light incident in the system can excite these s-like modes, that is elliptical modes with the electric field component mainly in the y direction, via the off-diagonal optic tensor terms. When this occurs there is a dip in the reflected intensity of p-polarised light.

It is seen that s–p mixing is observed more strongly through the surface plasmon-polariton resonance, since in this region there are large E fields present in the system due to the surface enhancement of the surface plasmon-polariton. In the region of the mainly p-like modes there is less energy coupled into the layer between the modes, and so less to couple into these s-like modes. The effect in the surface plasmon-polariton is illustrated by the E field plots in figure 6. These are shown for p-polarized incident light, at an angle in the surface plasmon-polariton resonance where the fourth s-like mode is excited. The E field in the y direction (E_y is shown in figure 6 (*a*). This does not show any surface enhancement but there is a strong E field oscillation across the layer due to the excitation of the s-like propagating mode. The E field in the z direction (E_z) is shown in figure 6 (*b*). This shows a strong surface enhancement due to the excitation of the surface plasmon-polariton, there is also a weak field oscillation across the layer.

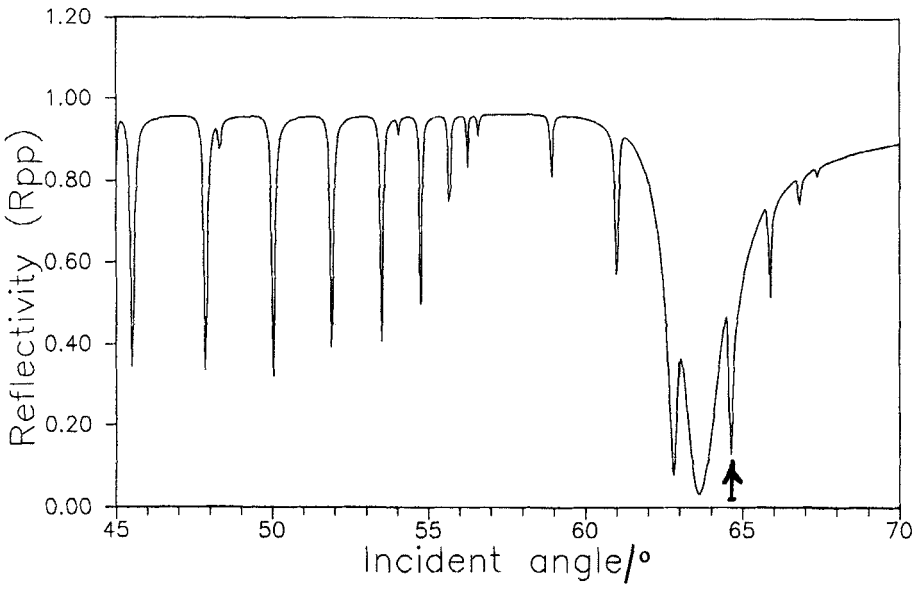

Figure 5. Reflectivity for p-polarized light for a system where the optic axis is tilted out of the plane of the cell surfaces, with the cell in the perpendicular orientation. The arrowed mode indicates the point at which the electric field distributions are shown in figure 6.

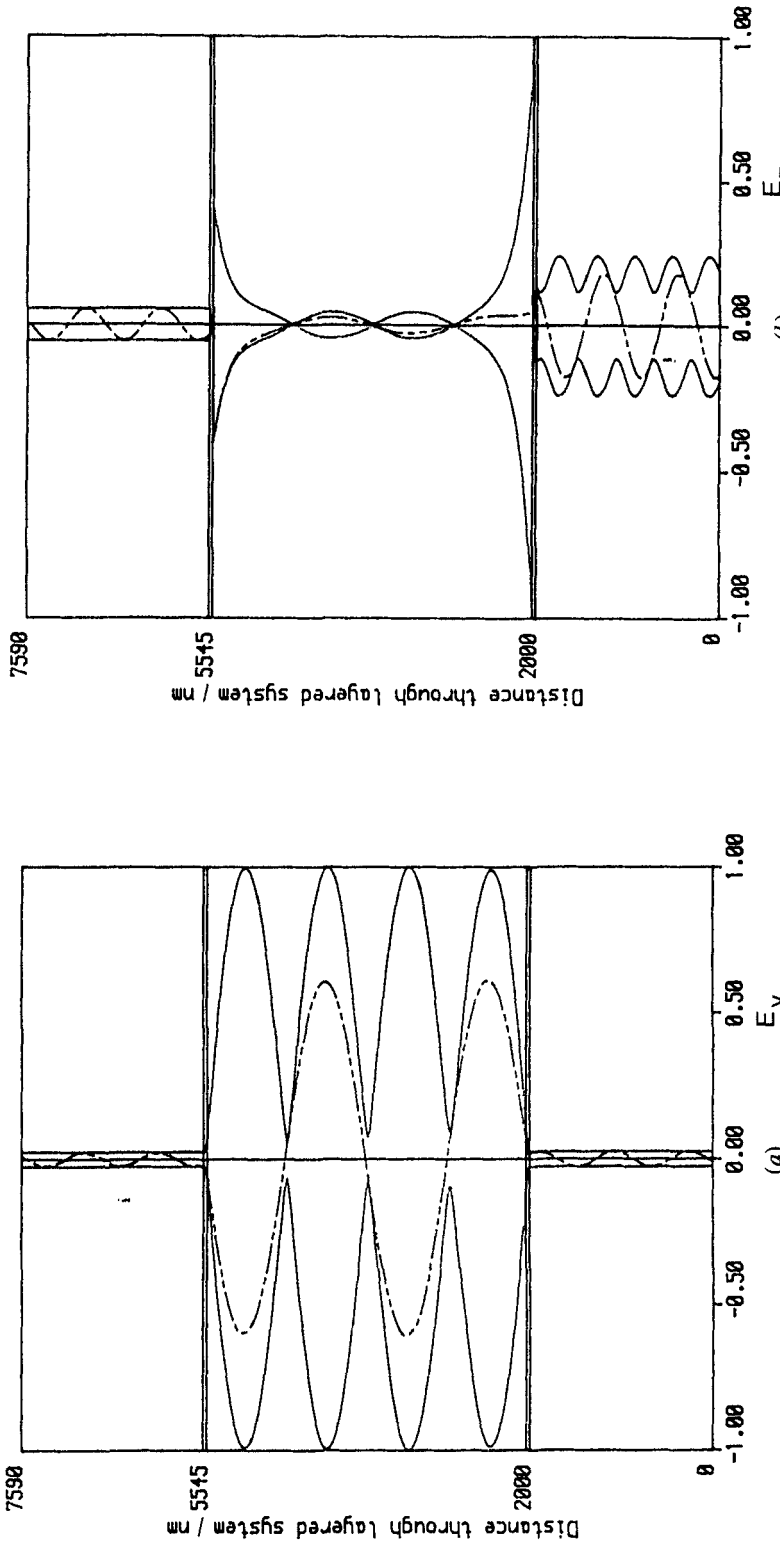

Figure 6. (*a*) A plot of the *y* component of the electric field (E_y) in a sample containing a tilted uniaxial slab of dielectric material. It is taken at the point of excitation of the fourth s-like mode in the perpendicular cell orientation, arrowed in figure 5, the incident radiation is p-polarized. The central portion of the figure is the gap containing the uniaxial slab; this is contained between the thin silver layers. The outer regions of the figure show the glass pyramids, the bottom of the figure is the incident pyramid. The continuous oscillatory line across the figure represents the amplitude of E_y, the dashed line shows E_y at some instant in time. The standing s-like mode is clearly seen across the sample, indicating the effect of the s–p mixing. Incident p-polarization, wavelength = 0·633 E − 6 m, angle of incidence = 64·65°; max. in CPT = 0·286 E 1. (*b*) A plot of the *z* component of the electric field (E_z) in a tilted uniaxial sample at the same point. The strong surface enhancement due to the excitation of the surface plasmon-polariton on the first silver surface is clearly seen. There is a weak oscillation across the sample, since the s-like mode is mixed. Also seen is a weak standing wave in the first pyramid, since some p-polarized radiation is reflected. Incident p-polarization; wavelength = 0·633 E − 6 m; angle of incidence = 64·65°; max. in CPT = 0·509 E 1.

So it is seen that the situation is now more complicated due to the broken symmetry. The observation and comparison to theory of such mixed modes can lead to important information about the tilt and twist etc. within the liquid crystal layer. In this example is seen that a uniaxial layer which is tilted from the plane of the surfaces leads to mixed modes in the perpendicular cell orientation, but not in the parallel cell orientation. Twist in the cell would, however, lead to a component of the optic tensor not orthogonalized in the xz plane when the cell is in the parallel orientation and hence s–p mixing would occur in this orientation as well.

Now, as a further example, observation of structure within the sample will be considered, that is variation of the optic tensor orientation as a function of z. To illustrate this the effect on the resonant mode structure of the addition of a thin layer of different orientation in the middle of the cell will be shown. The previous system considered was a uniform uniaxial layer tilted by a few degrees. Now a thin layer

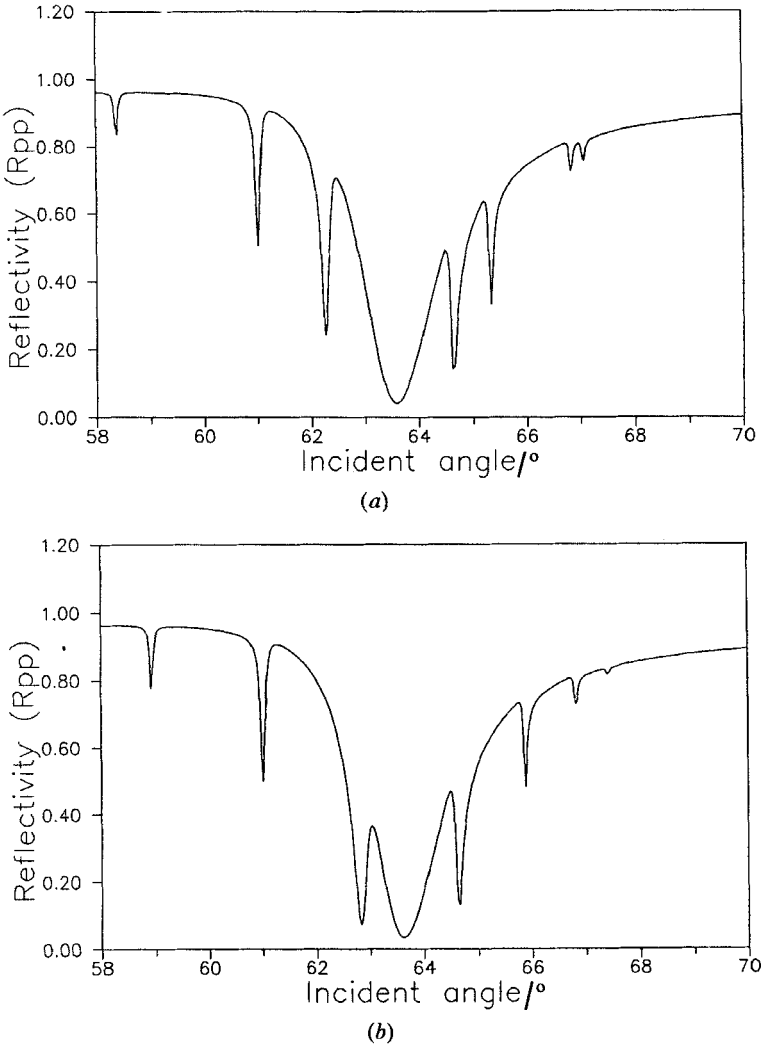

Figure 7. The reflectivity for a sample with an additional thin layer of different orientation in the middle of the cell (*a*), compared with that for a uniform alignment (*b*).

twisted by 90° about the z axis is inserted in the middle of the sample. The reflected intensity against angle through the surface plasmon-polariton resonance for this system for p-polarized incident light (R_{pp}) in the perpendicular orientation is shown in figure 7. This also shows an expanded reflectivity against angle plot for the surface plasmon-polariton for the simple tilted layer system as before. It is apparent that alternate s-like modes in the surface plasmon-polariton have been shifted in angle. The reason for this is clear when the electric field distribution within the layer is considered. As illustrated earlier the first mode (similar to TE_1) has one E field peak in the middle of the sample. This mode is, therefore, sensitive to the region of different alignment in the middle of the cell and so the angle at which it is excited changes. The second mode (similar to TE_2) on the other hand has an E field zero in the middle of the sample. This then is insensitive to the addition of the layer of different alignment and so is only displaced slightly in angle. Thus the alternate modes with an E field peak in the middle of the sample are sensitive to, and therefore displaced by, the addition of a layer of differing alignment in the middle of the cell. This argument can be extended to other regions within the layer of material. It is, possible, therefore, to use these excited modes with field peaks at differing positions within the layer of material under examination to investigate the way in which the optic tensor is configured through the system.

Having seen that the surface plasmon-polariton can couple into mixed polarization guided modes in the cell it is useful to consider its dependence on optic tensor orientation. The surface plasmon-polariton being associated with a surface charge density oscillation has the main E field component in the z direction. There are weak fields in the x-direction (that is the direction of propagation) however, as in the case of propagating p-modes. Due to the dominance of the field in the z direction the angle at which the surface plasmon-polariton is excited is very strongly dependent on the z component of the optic dielectric tensor (ε_{zz}). Small variations in the magnitude of ε_{zz} will cause large variations in the angle at which the surface plasmon-polariton is excited. This is a very useful property for the examination of surface tilt in liquid crystal materials. Clearly addition of surface tilt in an aligned liquid crystal with $\varepsilon_{\parallel}$ ($\approx n_e^2$) lying in the x direction say, will change the angle at which the surface plasmon-polariton is excited. In practice the situation is a little more difficult due to a lack of understanding of the SiO layer, this will be discussed more fully in the Experimental method section.

In the general case of some arbitrary optic tensor orientation in the cell within the surface plasmon-polariton penetration depth it is also possible to excite the surface plasmon-polariton with incident s-polarized light. This can then couple to the surface plasmon-polariton via s–p mixing due to the cross components in the optic tensor. This is also very useful for the examination of near surface twist and tilt in the cell.

3. Experimental method

The ferroelectric liquid crystal cell used in the experimental work is shown in figure 1. It is constructed from glass pyramids. These are used so that when the surface alignment direction is parallel to one of the pyramid edges it is possible to orient the cell and take the data with either the surface alignment direction parallel to or perpendicular to the plane of mode propagation. The pyramids are square based (with faces 2·5 × 2·5 cm) and made from high index glass of $n = 1{\cdot}8$ ($\varepsilon = 3{\cdot}24 + 0{\cdot}0i$) at 632·8 nm. Onto these thin layers of silver are vacuum evaporated. These are chosen to be of optimum thickness to couple well to a surface plasmon-polariton on the silver/liquid crystal interface and also form good reflective layers for resonant guided mode

propagation. The silver layers are characterized using the surface plasmon-polariton resonance. With the simple glass/silver/air system, incident p-polarized light can excite a surface plasmon-polariton on the silver/air interface. The form of the resonance depends on the dielectric constant and thickness of the silver film under investigation. By fitting a theoretically calculated reflectivity curve to that experimentally obtained it is possible to determine ε and the film thickness [12]. Such a fitted reflectivity curve is shown in figure 8; the results for this film are,

$$\varepsilon = -17{\cdot}62(\pm 0{\cdot}03) + 0{\cdot}71i(\pm 0{\cdot}03i) \quad \text{and} \quad t = 46{\cdot}5\,\text{nm}\,(\pm 0{\cdot}5\,\text{nm}).$$

The dip in the reflectivity below 33·75° is due to weak direct transmission through the silver film below the critical angle between the glass and air. Now onto the pyramids with thin silver films thin layers of silicon monoxide are evaporated to form alignment surfaces for the liquid crystal. These are evaporated at 60° angle of incidence in order to form a homogeneous nematic alignment with the director perpendicular to the plane of SiO evaporation. The thickness of the SiO layer is $\sim$20 nm, as determined by the change in frequency of a quartz crystal oscillator, with the crystal placed in the evaporation beam. This layer is a little more difficult to characterize than the silver. For thin overlayers of dielectric material on the silver the position of the surface plasmon-polariton resonance will be displaced in angle. However the displacement will depend on the optical thickness of the layer, that is $\sqrt{\varepsilon'} \times$ thickness. It is, therefore, necessary to model this layer with an assumption about its thickness. With the layer thickness assumed to be 20 nm (as determined at the time of evaporation) fitting a theoretical curve to the new surface plasmon-polariton resonance data leads to a value of the dielectric constant for the SiO layer of, $\varepsilon \sim 2{\cdot}65(\pm 0{\cdot}01) + 0{\cdot}001i$. If the assumed thickness is too large then the determined value of ε will be too small, and vice versa. Here, however, due to the rough surface of the SiO (which gives it its liquid crystal aligning properties) this value cannot be compared to the bulk value for SiO to check the result.

Having characterised the silver and SiO layers the pyramids are assembled together in a clean room with thin mylar spacer strips to form the liquid crystal cell. In general the assembly is with the evaporation directions of the SiO layers parallel. Comparison

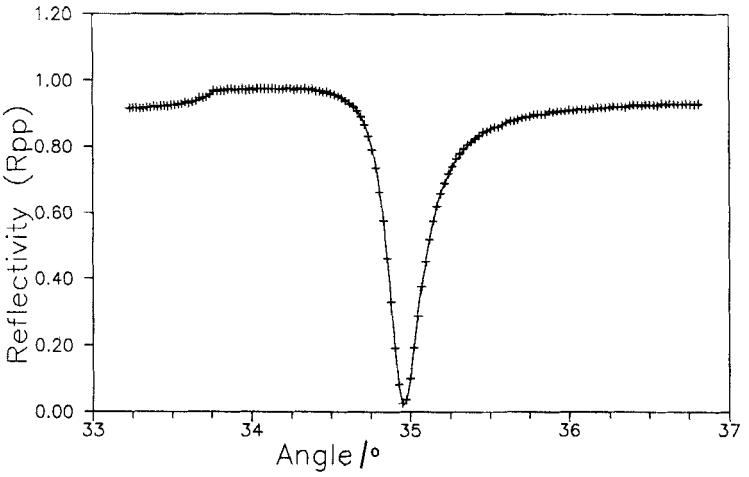

Figure 8. Fitted R_{pp} curve for a thin silver film on a pyramid. The crosses are the data and the line is a theoretical fit.

of cells with parallel and anti-parallel evaporated SiO, however, does not reveal any difference as the surface pre-tilt, in an SiO aligned cell where the SiO is evaporated at 60° incident angle, is zero. This whole cell is then placed in a temperature controlled oven which is stabilized to $\pm 0{\cdot}1$°C using a differential feedback unit, monitoring the temperature in the oven cavity. The size of the pyramids forming the cell help to stabilize the temperature of the cell, so any temperature fluctuations in the liquid crystal layer itself will be both small and slow. The cell temperature is measured directly with a thermocouple attached to one of the pyramids with thermal grease. Temperatures quoted here have a relative accuracy of $\pm 0{\cdot}1$°C, but absolute accuracy of only ± 1°C. The cell in the oven can be heated to a temperature in the isotropic phase of the liquid crystal used and capillary filled. The oven allows control of the temperature of the cell across the range of phases of interest, down to room temperature.

In order to record the data in the required form of reflectivity as a function of angle of incidence the cell in the oven is placed on a computer controlled rotatable table. The experimental arrangement is shown in figure 9. The cell is illuminated with a He–Ne laser light source at 632·8 nm, which is chopped at about 2 kHz to allow phase sensitive detection giving high signal to noise ratio. The beam is arranged to be either p- or s-polarized. A reference beam is taken in order to allow drift in the laser intensity to be compensated for. The laser beam passes through the cell in the oven and into the signal detector. This detector is geared to the table on which the cell is mounted in such a way as to move through twice the angular displacement of the sample, thereby tracking the reflected beam. Computer control of the table gives movement in steps of 0·01°, although absolute positional accuracy is limited to about 0·03°. The signal is recorded on computer and divided by the reading from the reference beam detector. Data are corrected in the computer to allow for the beam refraction at the air/pyramid interfaces. Also the reflectivity at the air/pyramid interfaces is corrected for using appropriate formulation of Fresnel's equations. The true reflectivity as a function of internal angle of incidence for the light incident on the glass/liquid crystal interface is thus obtained. With this data we now need to find a satisfactory model of the system.

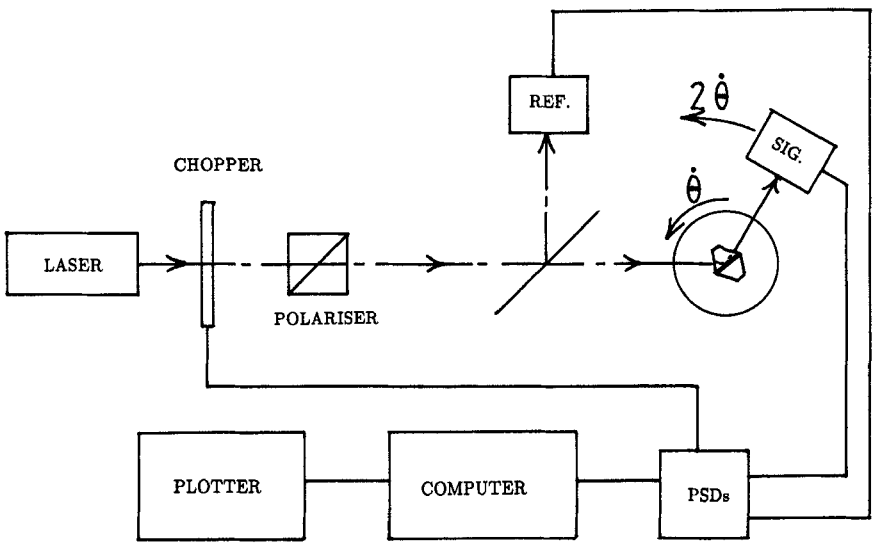

Figure 9. The experimental arrangement used to take the data presented in this work.

The most elegant solution to the problem of obtaining the actual optic tensor profile within a cell from the reflectivity data would be to directly transform between the data taken and the optic tensor configuration present. This is not, however, possible in practice. Hence the data obtained is analysed by comparison with theoretical calculations of the reflectivity curves. The continuous nature of the optic tensor distribution within the liquid crystal layer can be modelled by splitting the layer into many thin uniform sheets. Calculating the optical properties of each of these and matching the boundary conditions between successive sheets allows evaluation of the optic properties of the whole sample [11, 16, 17]. In the high temperature phases (isotropic, nematic and smectic A) the optic tensor configuration within the sample is well known. In the chiral smectic C phase however the optic tensor structure is not known and it is, therefore, necessary to guess first a possible profile. Comparison of predicted reflectivity curves from this profile with the data will establish whether it is a correct profile, and appropriate corrections to the model can be made. Using this method it is then possible to determine the optic tensor profile within the liquid crystal layer in the cell.

4. Results

The material used in the work presented here is the BDH commercial material SCE3. The transition temperatures supplied by the manufacturers are

$$C\ -15°C\ S_C^*\ 72{\cdot}4°C\ S_A\ 102{\cdot}7°C\ N^*\ 134{\cdot}4°C\ I$$

This is therefore a practical ferroelectric liquid crystal for display purposes since it is in the S_C^* phase at room temperature. The spontaneous polarization (P_s) at room temperature is quoted as $8\,nC\,cm^{-2}$. The tilt or cone angle is given as 24° and the optical birefringence is quoted as 0·18. These parameters were measured using conventional techniques and so they may be subject to some error due to the lack of understanding of the optic tensor and smectic layer structure in a cell containing the material. The values obtained here for some of these parameters may, therefore, be expected to vary from those quoted. The pitch of the helical structure in the N* phase is $>30\,\mu m$, so no problems in alignment should occur in thin cells (less than $\sim 7\,\mu m$) where the surface alignment should suppress the chirality, since the N* phase should unwind in a cell which is less than 1/4 of a pitch in thickness.

Pyramids are prepared and coated with silver and SiO layers for the cell construction. The silver and SiO layers having been characterized as described earlier, a cell is constructed with $3{\cdot}5\,\mu m$ mylar spacers. This is then heated in the temperature stabilized housing on the experimental arrangement to a temperature in the isotropic phase of the material (i.e. >134·4°C). This being set at about 140°C introduces a rather severe problem. There is a tendency for the silver to anneal significantly and its dielectric parameters to change. There is also some reaction between the SiO and silver which tarnishes the silver/SiO surface. This, of course, alters the surface plasmon-polariton resonance, causing it to become very broad in angle and rather shallow. Also the guided mode resonances become weaker due to the lowering of the Q of the cavity. In order to alleviate this difficulty it is necessary to remain in the isotropic phase temperature region of SCE3 for only a brief time. Therefore, once the temperature of 140°C is reached the cell is filled, introducing the SCE3 material at the bottom of the cell and allowing capillary action to draw it in. The entrance of the material into the cell can be observed quite easily, despite the presence of the silver layers preventing direct observation. If the cell is observed such that the internal angle of incidence (i.e. angle of

incidence with the glass/silver surface) is approximately the surface plasmon-polariton angle for the cell filled with isotropic liquid crystal (that is $\sim 65°$), then as the material enters the cell a colour tinge is observed on the silver surface. This is due to the absorption of light by the surface plasmon-polariton. Once the cell is filled the oven temperature is immediately reduced to a point low in the N* phase ($\sim 110°C$). In this way the sample only stays in the temperature region of $> 120°C$ for about half an hour. Thus degradation of the silver is minimized, the surface plasmon-polariton resonance remaining sharp and deep after the introduction of the liquid crystal.

In order to form a foundation to the investigation of the optic tensor structure in the S_C^* phase of SCE3, and to illustrate the techniques involved, initially the structure in the higher temperature N* and S_A phases is examined. In both of these cases the data should be well modelled by a simple uniaxial slab, providing the data is taken in a region free from defects. Reflectivity against angle of incidence data can be taken as described in § 3. Such data for incident p-polarised light with the nematic surface alignment direction parallel to the plane of light propagation are shown in figure 10 (as crosses) for a cell temperature of 109°C. The angle range is dictated by experimental constraints, set by the oven used in the temperature control of the experiment. Clearly the data show the features expected, with resonant guided modes and a broad surface plasmon-polariton resonance dip for p-polarized light (R_{pp}), (only a series of guided mode dips would be seen for s-polarized light (R_{ss})). The R_{ss} data (not shown) can be fitted using the multi-layer modelling techniques, fixing the parameters for the silver and SiO layers at those obtained before the cell is assembled. In this configuration this leads to the determination of the sample thickness and the dielectric constant at optic frequencies, perpendicular to the nematic director. For this sample the thickness is $3{\cdot}57\ \mu m$ and $\varepsilon_\perp = 2{\cdot}190 + 0{\cdot}001i$; the thickness of the sample is accurate to $\pm 0{\cdot}02\ \mu m$. If the thickness in the theoretical calculation is varied from the value obtained by more than this amount then there is a noticeable displacement between the position of the guided modes in the theory and data. This is particularly so for higher mode number (lower angle). The ε' value is accurate to $\pm 0{\cdot}003$, leading to an n_0 of $1{\cdot}480 \pm 0{\cdot}002$. The accuracy of ε' is limited not only because of the error bounds on fitting the data, but also due to the limit in accuracy to which the incident angle of the light is known. (i.e. The ability to set zero on the rotary table, which is correct to $\pm 0{\cdot}02°$). This, however, has only a second order effect on the thickness obtained, which is determined by the mode spacing rather than absolute angle. The value of ε'' is unfortunately rather unreliable. When the sample is constructed with the mylar spacers and clamped together it is almost impossible to obtain absolute uniformity of cell gap over the whole cell area. The laser beam used to probe the cell is of finite area, and therefore samples a range of cell thickness. This range of cell thickness causes a broadening of the resonant modes. This has, therefore, a similar effect to a higher value of ε'', i.e. higher absorption in the liquid crystal layer. These effects are not totally degenerate however. Wedging causes a broadening of high order modes, while a large ε'' causes all modes to be broadened. It is, difficult, however, to distinguish fully between variation in sample thickness and absorption in the liquid crystal layer for a well aligned cell. The value obtained in fitting the R_{ss} data is $\varepsilon'' = 0{\cdot}001$, and this will be used here.

An initial fit to the R_{pp} data is shown by the continuous line in figure 10. The fit is obtained by locking the thickness of the cell and varying $\varepsilon_\parallel$ and $\varepsilon_\perp$ as the fitting parameters and fitting to the p-polarized guided modes. Since the material in the nematic phase is uniaxial the value of $\varepsilon_\perp$ obtained should be within the error bounds of the value obtained fitting the R_{ss} data. This is the case, since fitting leads to values of

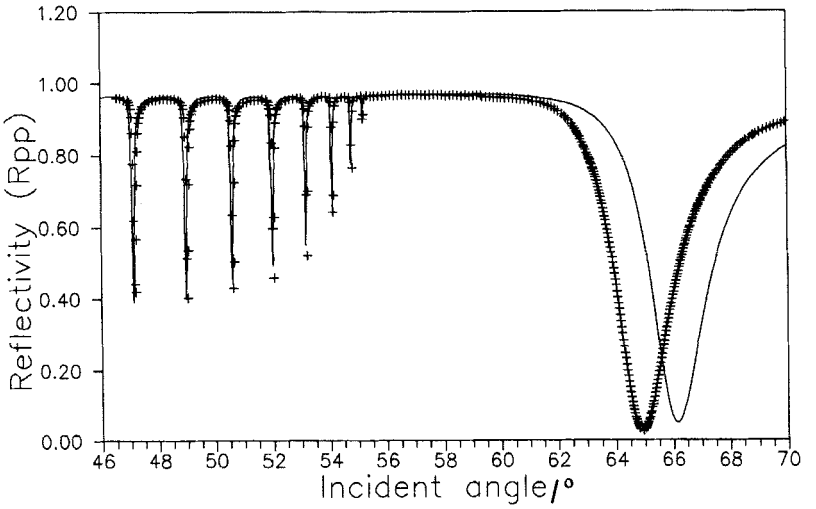

Figure 10. Initial fit to R_{pp} for SCE3 in the N* phase at 109°C. Data are the crosses, theoretical fit is the continuous line. Fit is dictated by the resonant guided modes.

$\varepsilon'_{\|} = 2{\cdot}692$ and $\varepsilon'_{\perp} = 2{\cdot}191$. Quite clearly there are serious problems with the surface plasmon-polariton resonance. With the silver and SiO parameters found by fitting the surface plasmon-polariton resonance before the cell was assembled, and the liquid crystal parameters obtained by fitting the s and p resonant guided modes it is expected that the surface plasmon-polariton resonance should automatically be correct, as there are no other free parameters present. (Although there will be an increase in the value of ε'' for silver due to the elevated temperature, which could have a small effect on the width of the surface plasmon-polariton resonance.) There are however reasons why the surface plasmon-polariton may not fit. Heating the sample is known to affect the silver and/or SiO dielectric parameters. This can be clearly seen by taking the empty cell through a cycle of heating and cooling, taking surface plasmon-polariton resonance curves before and after. However, this is done quickly here (in order to fill the cell), and experimentation has shown that the effect on the silver and SiO dielectric parameters (and hence the surface plasmon-polariton) is not significant. Alternatively the porous nature of the SiO surface may be interpenetrated by the liquid crystal material and this could cause a variation in the effective SiO dielectric parameters. This has been observed before by Innes [18] and seems to be the explanation for the effect observed here. It is necessary, therefore, to adjust the SiO dielectric parameters after the cell has been filled in order to fit the surface plasmon-polariton resonance dip correctly. Changing the SiO optical dielectric constant from $\varepsilon = 2{\cdot}65 + 0{\cdot}001i$ to $\varepsilon = 2{\cdot}49 + 0{\cdot}001i$ leads to the fit to the R_{pp} data shown in figure 11; this is now a very acceptable fit to the data. It may now be reasonably asked if the surface plasmon-polariton resonance is relevant, since there is a need to adjust the SiO parameters in order for the theory to fit the surface plasmon-polariton data. However, it has been seen that the surface plasmon-polariton couples strongly to s-like modes if there is some twist/tilt structure in the optic tensor profile in the cell and the value of this will be seen in the work on the S_C^* phase.

It is seen from the fit to the R_{pp} data in figure 11 and the fitting to the R_{ss} data (not illustrated) that this material in the nematic phase can be modelled, as expected,

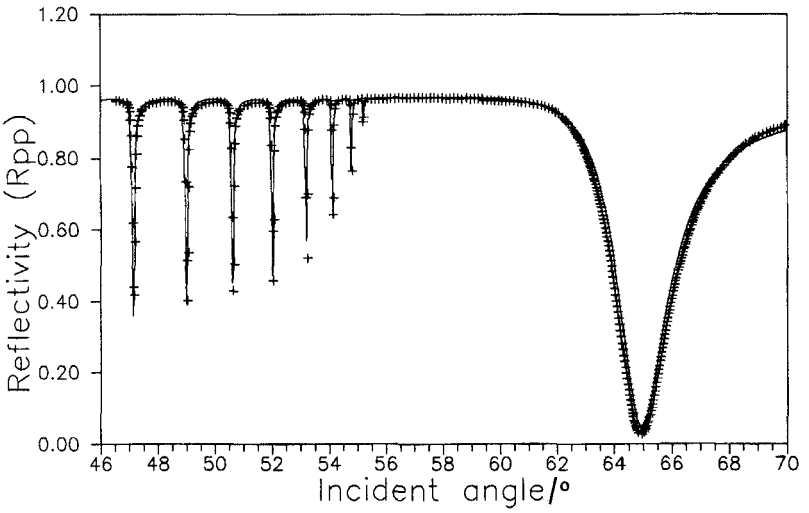

Figure 11. Improved fit to the data for SCE3 in the N* phase, obtained by correcting the SiO dielectric parameters for liquid crystal interpenetration. Data are the crosses, theoretical fit is the continuous line.

satisfactorily with a simple uniaxial slab of dielectric material with optic axis parallel to the surface alignment direction. The fits are of a good quality, and information on the cell thickness and corrected value of the SiO layer dielectric constants are obtained.

It is interesting to note that if the cell was assembled such that the surface alignment directions on the front and back pyramids were not quite parallel this would manifest itself as s–p mixing in the data. The variation in twist angle across the cell means that there would be a component of the optic tensor which is not orthogonalized in the plane of light propagation, thus giving s–p mixing. The lack of s–p mixing means that cells are assembled which have front and back alignment directions which are parallel to within $\sim 1°$. The cell can now be cooled to examine the situation in the S_A phase. Reflectivity data taken in the S_A phase for a well aligned sample has the same form as data taken in the N* phase. This does not always occur however, and sometimes a poorly aligned S_A phase forms. This is probably due to slight misalignment of the surface alignment directions on the faces of the pyramids forming the cell, leading to a slight splay of the director in the nematic phase. Then the formation of the smectic layers, which are perpendicular to the director in the S_A phase, introduces disclinations which broaden the guided modes in the reflectivity data. This effect is seen as lines growing across a cell in the S_A phase if it is observed between crossed polaroids in the conventional manner. Fitting the data taken for a well aligned cell in the S_A phase leads to the liquid crystal parameters and cell thickness in this phase. For example, at 72·8°C $\varepsilon'_\perp$ (n_o^2) at optical frequencies (He–Ne 632·8 nm) is $2{\cdot}208 \pm 0{\cdot}003$ and $\varepsilon'_\parallel$ (n_e^2) is $2{\cdot}760 \pm 0{\cdot}003$. The absorption ($\varepsilon''$) remains the same at about 0·001, cell thickness is now 3·55 μm. Again it is seen that the data can be well fitted with a simple uniaxial slab model.

Having examined the response of the sample in the N* and S_A phases, and seen that the data and results from fitting this data correspond well with that expected, the sample can now be cooled into the S_C^* phase and the structure formed can be examined. The sample is cooled very slowly across the S_A to S_C^* phase transition in order to obtain

monodomains of uniform optic tensor orientation sufficiently large to examine. This process is helped by the thermal inertia of the glass pyramids forming the cell walls, which give a degree of thermal stability to the liquid crystal layer. The rate of temperature change across the phase transition is then limited to about 0·5°C/h. At a temperature just in the S_C^* phase of SCE3 at 70·2°C data taken with p-polarized light (R_{pp}) with the sample oriented such that the surface alignment direction in the nematic phase is parallel to the plane of light propagation (parallel cell orientation) is shown in figure 12. This shows only the guided mode region of the data, since there is no perceptible change in the surface plasmon-polariton resonance across the phase transition. Careful examination of this data reveals that it is slightly different from that taken just above the transition temperature which is similar to that for the nematic phase shown in figure 11. In addition to the series of sharp, deep p-polarized resonant guided modes seen before there is an additional set of much weaker modes. Comparison of R_{pp} data with R_{ss} data taken at the same temperature reveals that these modes are at the positions where s-modes are excited. This shows that s–p mixing is occurring, and the guided modes are no longer either purely p-polarized or s-polarized but are weakly mixed elliptical modes. This effect is seen more clearly if data are taken with crossed polaroids. Here the probe beam polarizer is set to p-polarization, and the detector is set to detect reflected s-polarized light, (these data are termed R_{ps}). R_{ps} data are shown for this sample at 70·2°C, just in the S_C^* phase, in figure 13. Here spikes are seen where either a p- or s-like mode is excited, and a low background signal (s–p mixing intensity) elsewhere. This is because when a mode is excited, either p-like directly or s-like via s–p mixing, then s–p mixing causes the reflected beam to be elliptically polarized, which hence has a s-polarized component. This clearly shows the mixed nature of the modes excited in this phase.

This introduction of s–p mixing in the parallel orientation of the sample indicates that there is some twist present in the cell. In order for s–p mixing to occur there must be some component of the optic tensor not orthogonalized in the plane of light

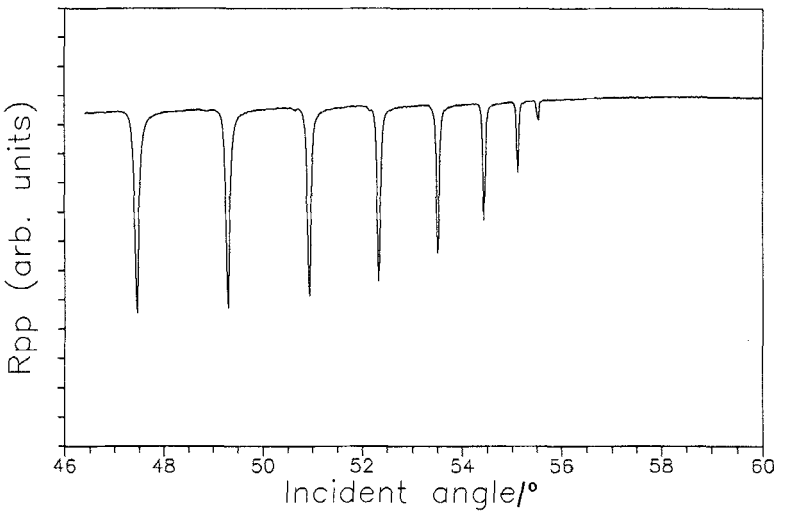

Figure 12. Reflectivity data for p-polarised light in the guided mode region with the cell in the parallel orientation, at a temperature of 70·2°C, just in the S_C^* phase.

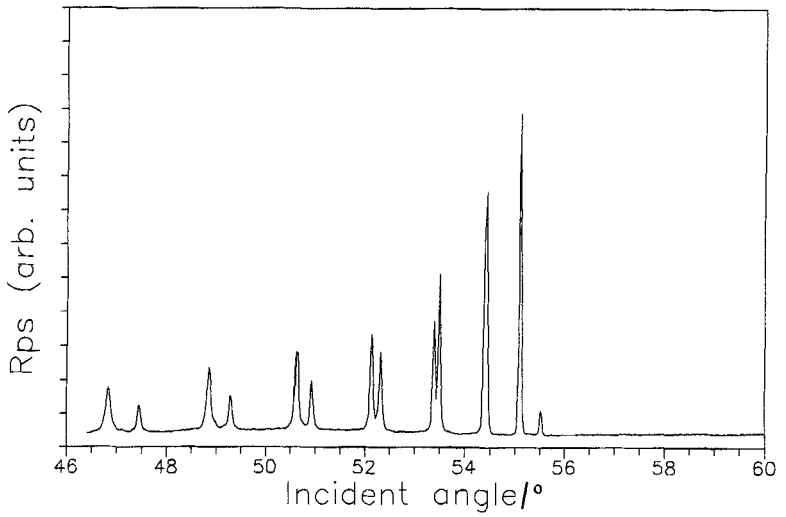

Figure 13. Reflectivity data for input p-polarized light observing s-polarized reflected light (R_{ps}) with the cell just in the S_C^* phase as in figure 12.

propagation. Assuming that the optic dielectric tensor has remained uniaxial across the phase transition, then for the parallel cell orientation, tilt of the optic tensor does not cause this, since in this orientation this leaves the optic axis in the xz plane. Twist, however, takes the optic axis out of the xz plane and therefore, since s–p mixing is seen twist must occur. This is quite obvious from the observation of conventional cells, where when the S_A to S_C^* phase transition is crossed the extinction angle for a cell observed between crossed polaroids is seen to twist from the surface alignment axis.

If the sample is rotated by 90° about the z axis such that the surface alignment direction is perpendicular to the plane of light propagation (the perpendicular cell orientation) then the results are a little different. Here the region of the p-polarized guided modes does not show any significant s–p mixing. The R_{pp} guided modes look the same as in the S_A phase, only being displaced slightly due to the small changes in the optic tensor dielectric constants with the small decrease in temperature. The region of R_{pp} data through the surface plasmon-polariton resonance does, however, show weakly mixed modes (similar to those seen in figure 5). The mixed modes in the surface plasmon-polariton are s-like modes which extend through the surface plasmon-polariton region due to the higher value of $\varepsilon'_{\|}$ (n_e^2) and are excited via s–p mixing. Since this mode mixing is observed through the surface plasmon-polariton resonance some twist and/or tilt of the optic tensor must occur within the penetration depth of the surface plasmon-polariton, here this is about 0·3 μm [12].

Now it must be considered whether this data just below the S_A to S_C^* phase transition can be used usefully to determine the way in which the optic tensor configuration forms across the cell, i.e. is the weak s–p mixing observed, and the small perturbation on the position of excited modes just below the S_A to S_C^* transition sufficient to determine uniquely the optic tensor profile present within the sample? This is, unfortunately, found not to be so. In this situation there exists some small twist and possibly some small tilt within the cell. However since the amount of twist/tilt is no more than a few degrees the s–p mixing seen in the data is weak. It is very difficult,

therefore, to determine the precise nature of the twist/tilt profile across the ferroelectric liquid crystal layer. As the cell temperature is decreased the strength of the s–p mixing seen increases. This is consistent with the observation in conventional ferroelectric cells that the twist angle increases with decreasing temperature, here causing an increase in the amplitude of the s–p mixing. Because of this the situation at room temperature will be examined, as this presents stronger s–p mixing, and hence it is hoped data which clearly distinguishes the optic tensor profile in the cell.

It is known that, for a low surface tilt alignment cell (as here), at room temperature the ferroelectric liquid crystal layer is not, in general, a monodomain. The layer can form with many domain walls, defects and disclinations. Since this is the case, how will this affect the data here? It is observed that when the laser probe beam is sampling a region which includes a disclination or domain wall then the resonant guided modes become rather broad. Consider the data shown in figure 14; this shows data taken at room temperature for a cell filled with SCE3, the cell was known to be of uniform thickness from the data taken in the N* and S_A phases. Hence the mess in the guided modes is due to the formation of disclinations etc. and resulting non-uniform optic tensor configuration over the area of the probing laser beam. Because of the finite probe beam size it is not possible to examine with the method used here the structure of domain walls and disclinations. The area within the probe beam must, therefore, be a monodomain, otherwise only an average of the structure is seen. Clearly then it is possible to identify the presence of domain walls etc. by the effect on the guided mode quality, and therefore to avoid them, but it is not possible to examine their precise nature. If the domains present in a cell are rather small it is possible to focus down the size of the probe beam spot from $\sim 1{\cdot}5$ mm to $\sim 250\,\mu$m. This does, however, introduce a higher level of beam divergence, which increases the angular width of the recorded resonances. (Here this is limited to $\sim 0{\cdot}05°$ by focusing from an initial beam diameter of ~ 1 mm at an aperture, with a focal length of ~ 1 m.)

Data taken at room temperature are now presented, this is for SCE3 at 21°C. R_{pp} data are shown, for the cell in the parallel and perpendicular orientations, in figure 15.

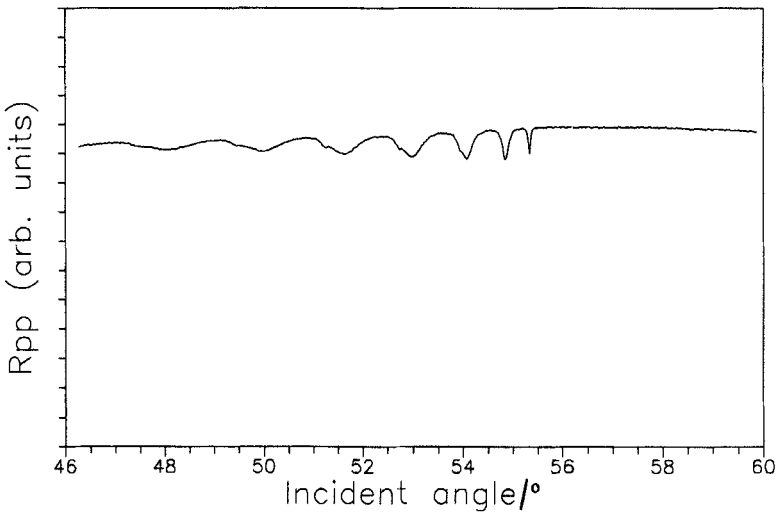

Figure 14. Reflectivity for a poorly aligned cell at room temperature. Area covered by the probe beam contains disclinations and this leads to weakly coupled optic modes in the film.

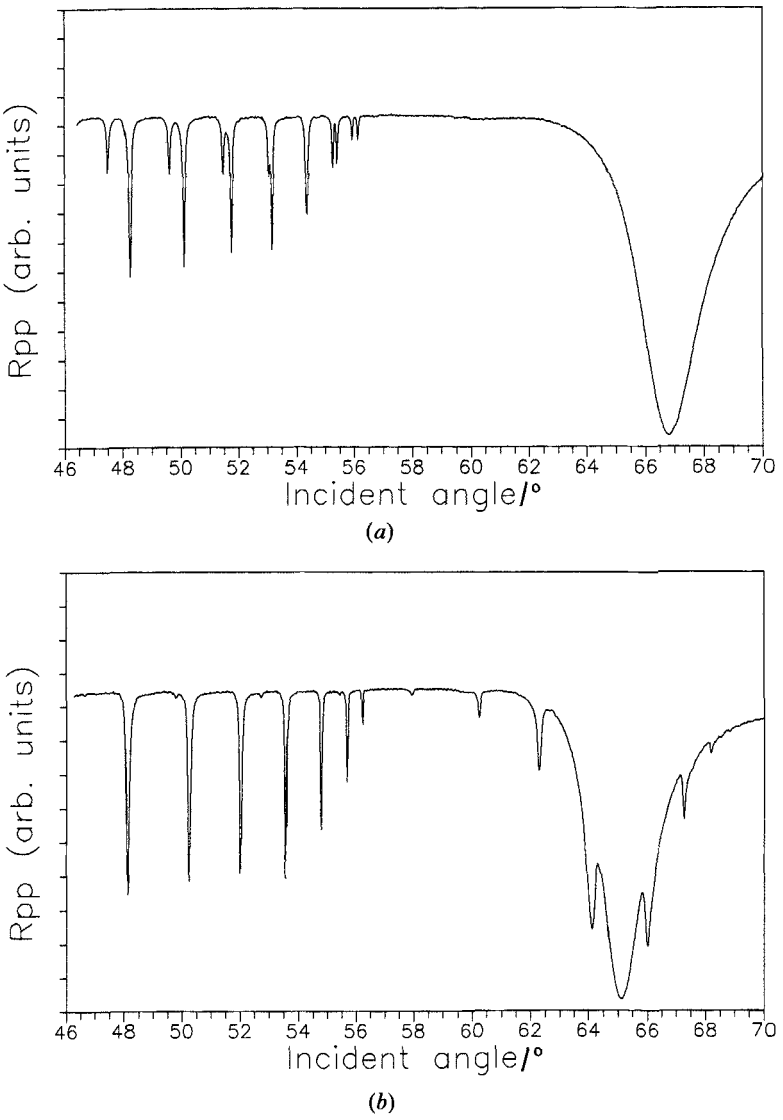

Figure 15. R_{pp} reflectivity data for (*a*) parallel orientation and (*b*) perpendicular orientation of the cell. The cell is at room at temperature in the S_C^* phase.

The form of these data is very similar to that seen just below the phase transition, however the strength of the s–p mixing is now greater, resulting in deeper mixed modes. It is hoped that this will lead to useful information on the optic tensor configuration within the ferroelectric liquid crystal layer. It is useful to note that the direction of the twist which is present in the ferroelectric liquid crystal layer can be determined by rotating the cell a few degrees about the z axis. If the rotation is towards the direction of the twist then the effective twist angle decreases and less s–p mixing results. If the rotation is away from the twist direction then the observed twist angle gets larger and the s–p mixing increases. In this way it is possible to determine the direction of the twist within the ferroelectric liquid crystal layer, even though it cannot be observed directly

due to the presence of the silver layers on the cell surfaces. Observation of the data shown in figure 15 immediately reveals that the s–p mixing in the guided mode region is much stronger in the parallel cell orientation than in the perpendicular cell orientation. Unfortunately this does not lead directly to information about the nature of the optic tensor profile in the cell. The effect is due to the different orders of s- and p-like modes excited in the two orientations. In the parallel orientation the p-like and s-like critical angles occur very close together and p- and s-like modes of a given order are excited at similar angles of incidence, thus there is a strong coupling between them. In the perpendicular orientation however p- and s-like critical angles are not close together, so modes of similar orders are excited at very different incident angles and a weaker coupling occurs.

There is now a problem in attempting to fit theoretical calculations to these data. In the I, N* and S_A phases the optic dielectric constants (or refractive indices) and the cell thickness were unambiguously determined from the fitting procedures, due to the simplicity of the optic tensor structure. Just below the S_A to S_C^* transition temperature it may well be possible to use extrapolated values. At room temperature this is not possible though, and the optic tensor parameters are more difficult to determine, since now the positions in angle of the resonant guided modes are not determined entirely by the optic dielectric constants of the material and the cell thickness. The optic tensor configuration within the liquid crystal layer will also affect the guided mode positions, and this is unknown and may be complicated. (This why the manufacturers quoted value for Δn of 0·18 may be in error, due to the lack of knowledge of the actual optic tensor profile within the layer.)

Observation of the room temperature data shows that the lowest order p-like mode in either orientation occurs at about 56·25°. The lowest order s-like mode in the perpendicular cell orientation (seen most clearly via the s–p mixing through the surface plasmon-polariton resonance in the R_{pp} data) occurs at approximately 68·25°. Now if this were a simple uniaxial slab of dielectric material aligned in the surface alignment direction, and the first mode corresponded to the critical angle for coupling into the liquid crystal layer, then since the pyramid index is $n = 1{\cdot}8$ this would correspond to optic dielectric constants of

$$\varepsilon'_{\perp} = 2{\cdot}24 \quad (n_o = 1{\cdot}50),$$

$$\varepsilon'_{\parallel} = 2{\cdot}79 \quad (n_e = 1{\cdot}67).$$

In the modelling these will be used as first approximations to the optic dielectric tensor, again initially ignoring biaxiality. The optic constants can then be varied to give the best fit to the data for any given proposed model of the optic tensor configuration within the ferroelectric layer. In this way any model can be optimized in order to evaluate whether it is correct and leads to reflectivity curves of the same form as the data taken. Then models for the optic tensor profile across the ferroelectric layer in the cell can be proposed and tested by modelling the theoretical reflectivity forms expected, and comparing with the data taken.

When ferroelectric liquid crystal materials were first studied in the thin cell geometry to form electro-optical devices [2] it was assumed that the smectic layering which formed in the S_A phase perpendicular to the cell walls was retained in the S_C^* phase. Then with the smectic layers held in this perpendicular configuration which is perpendicular to the nematic surface alignment direction the optic tensor profile is forced to take on some consistent configuration, this is the so-called bookshelf geometry. Within this system it would seem most favourable that the optic tensor

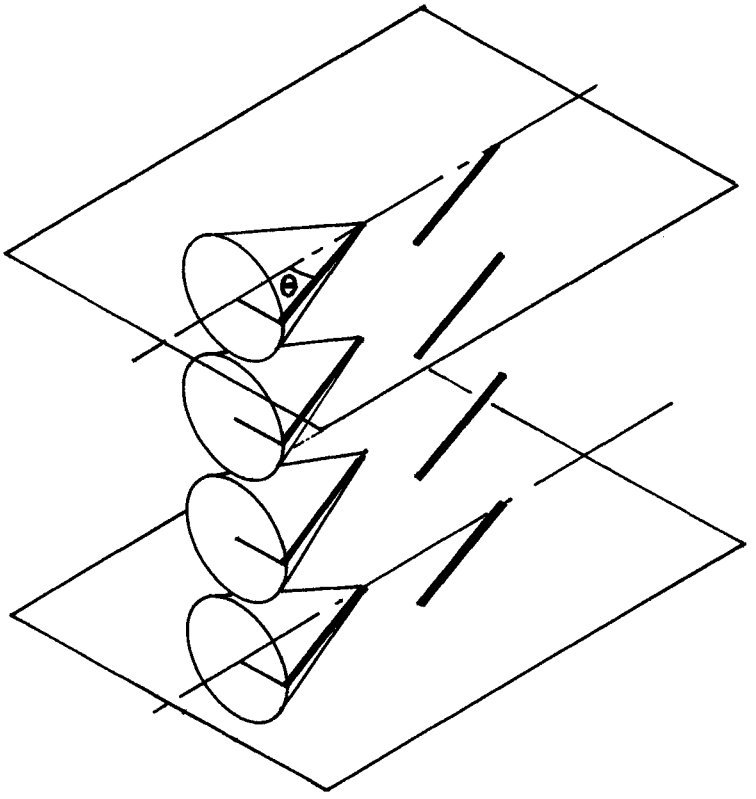

(*a*)

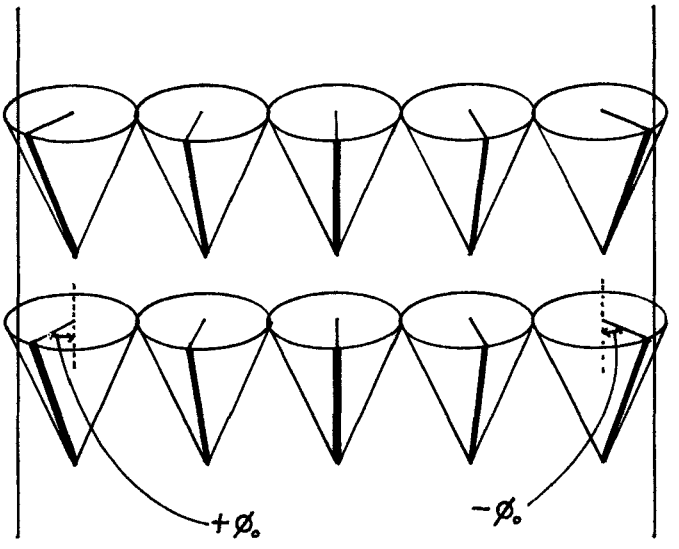

(*b*)

Figure 16. Schematic diagram of the bookshelf model, the heavy line indicating the optic axis. (*a*) Uniformly aligned as originally proposed and (*b*) including a finite surface pre-tilt.

major axis (for a uniaxial system this is also the optic axis, and corresponds to the mechanical director in higher temperature phases) lies in the surface plane. The resulting profile would be as illustrated in figure 16 (*a*). The formation of this structure, in addition to the smectic layering assumption, assumes that the surface anchoring energy in the alignment direction is small compared with the in-plane anchoring energy, i.e. it is easier to twist the mechanical director out of the surface alignment direction than to tilt out of the surface plane. This model is then equivalent to a uniform uniaxial slab of dielectric material with the optic tensor major axis twisted by the cone angle θ about an axis perpendicular to the cell surfaces (the z axis). Modelling the cell in this way with the room temperature cone angle for SCE3 of $\theta = 24°$ leads to a reflectivity curve for R_{pp} as shown for example in figure 17, with the cell in the perpendicular orientation. Comparison of this with the data shown in figure 15 reveals a considerable difference. Adjustment of the optic tensor dielectric component values does not account for the discrepancy between the data and the theoretical R_{pp}. It is therefore concluded that this simple uniform slab bookshelf model does not explain the data taken and is not a reasonable model of the optic tensor profile present within the cell. This is exactly to be expected from observation of conventional cells built from glass plates. The bookshelf model used here with a uniform slab of uniaxial material twisted from the alignment direction by the cone angle of 24° would lead to extinction angles between crossed polaroids for the two states of $\pm 24°$. In reality the extinction angles observed for a cell of approximately 3 μm thickness are much less than this, being just a few degrees. Any proposed model of optic tensor profile must be consistent with this simple observation.

In order to explain the lower than cone angle extinction observed between crossed polaroids Takezoe *et al.* [19] introduced the concept of surface pre-tilt into their modelling. A model of this nature is illustrated in figure 16 (*b*). Here the azimuthal angle ϕ is non-zero at the cell surfaces, being $+\phi_0$ at one surface and $-\phi_0$ at the opposite surface. The optic tensor then rotates smoothly between these values across the sample,

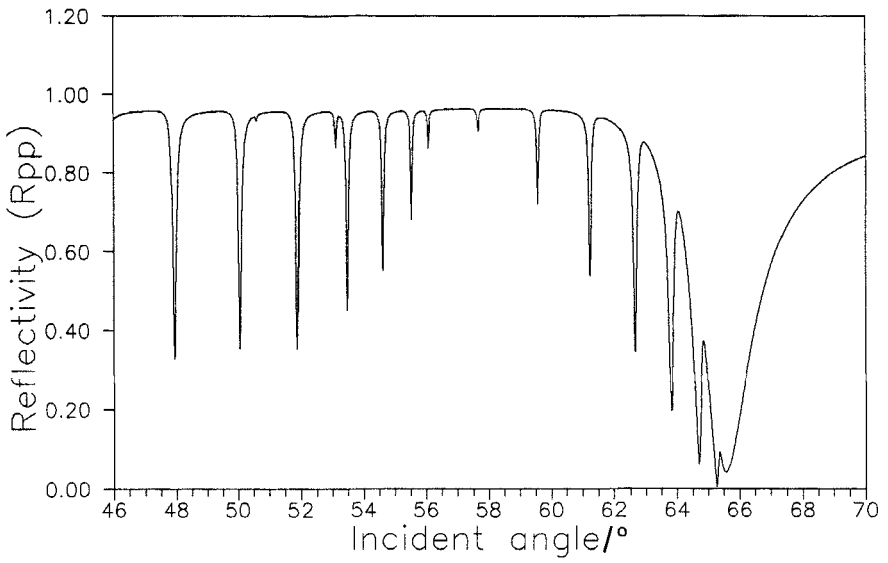

Figure 17. Theoretical reflectivity curve for the uniform bookshelf model with the cell in the perpendicular orientation.

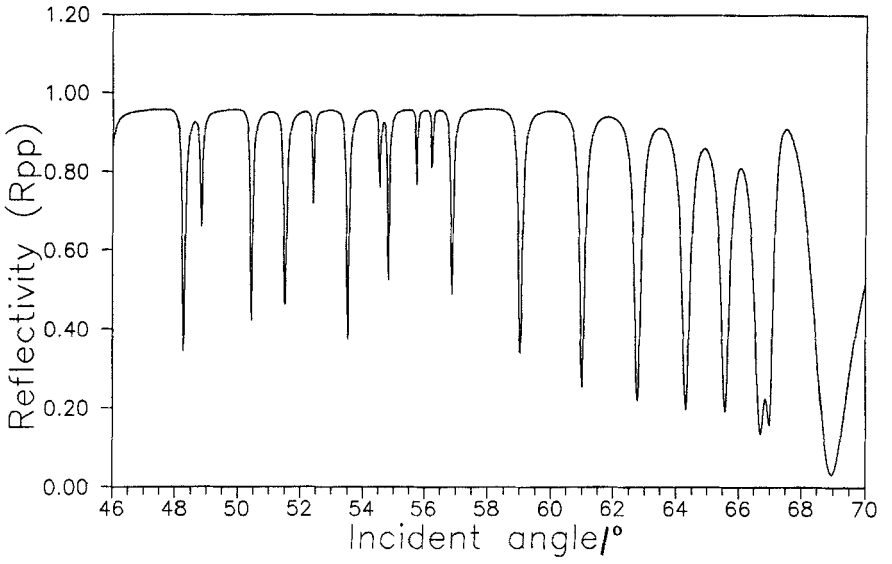

Figure 18. Theoretical reflectivity curve for the bookshelf model with the inclusion of a surface pre-tilt ($\phi_0 = 66{\cdot}7°$).

being constrained to move upon the cone within the perpendicular bookshelf smectic layering. Now let it be assumed that the twist angle at the surface of the cell should be about 10°. This would then lead to a realistic extinction angle between crossed polaroids for a conventional cell if the light were guided by the variation in twist within the cell, as in a twisted nematic cell. The light may be guided with the twist out to the cone angle in the middle of the ferroelectric liquid crystal layer and back to the surface twist angle at the opposite surface, leading to an apparent lower twist angle. (This, of course, cannot be directly examined here, due to the presence of the silver films on the pyramids which prevent direct observation of the system). With a cone axis tilt in the bookshelf model of $\delta = 0$ and a cone angle of $\theta = 24°$, this leads to an azimuthal angle ϕ_0 at the surface of 66·7°. So the bookshelf model with surface pre-tilt to give a surface twist of 10° can be modelled by allowing the azimuthal angle ϕ to vary from 66·7° to $-66{\cdot}7°$ across the liquid crystal layer.

Figure 18 shows a theoretical reflectivity curve for this model for R_{pp} with the cell in the perpendicular orientation. Again comparison of the theoretical curve with the data shown in figure 15 shows considerably disparity. Variation of the value of the surface pre-tilt and the optic tensor dielectric constants in this model shows that this is also not a good description of the situation present in the cell under examination. The s–p mixing through the surface plasmon-polariton resonance in the perpendicular orientation is clearly much too strong. Since the optical E field in the surface plasmon-polariton resonance is largely perpendicular to the cell surfaces, the large surface tilt leads to a strong coupling between the surface plasmon-polariton and s-like guided modes. This therefore indicates that the large surface pre-tilt in this model is incorrect, and therefore this model is also flawed.

Comment on bookshelf models

In the bookshelf type models proposed, with rigidly held smectic layering as formed in the S_A phase, the theoretical reflectivity curves do not compare well

with the data shown in figure 15. In each case the strength of the s–p mixed modes is clearly too great in the theoretical curves compared with the data. The mixed guided modes are too deep and the s-like modes extending through the surface plasmon-polariton resonance in the perpendicular cell orientation are too strongly excited. Also, even after optimization of the optic tensor values the mode positioning is incorrect, leading to poor correlation between data and theory. All models of the bookshelf type are therefore to be eliminated.

Having discounted simple bookshelf models as being inadequate to explain the data observed, leading to too much s–p mixing and modes which are excited at incorrect angles, we now go on to consider what are termed here banana models. In these the smectic layers are allowed to bend across the sample in some manner [20]. Consider the bookshelf model proposed before, with a surface pre-tilt such that the azimuthal angle ϕ_0 at the surfaces is $\pm 90°$. Now it seems intuitively unlikely that the layering formed in the S_A phase will be held rigidly when the material enters the S_C^* phase. Therefore, it is perhaps possible that the smectic layering bends to allow the major axis of the optic tensor (corresponding to the mechanical director) to lie in the surface alignment direction parallel to the cell surface at the surfaces. Then with $\phi_0 = \pm 90°$ at the surfaces the layer tilt angle δ at the cell surfaces would be equal to the cone angle θ. This model assumes that the surface anchoring energy is sufficient to retain the mechanical director (equivalent to the optic tensor major axis in the uniaxial approximation) in the surface alignment direction of the higher temperature phases. The optic tensor configuration for such a model is illustrated in figure 19 (*a*). The azimuthal angle ϕ is $\pm 90°$ at the surfaces, and rotates between the two across the layer of ferroelectric liquid crystal material. The smectic layers bend, keeping the optic tensor axis approximately parallel to the cell surfaces. (In this model the two switched states would be with the dipole pointing up or down in the centre of the cell.) This model also explains the relaxation observed after switching [21]. When a field is applied across the sample, the optic tensor would tend to rotate about the cone to the $\phi = 0°$ or $180°$ positions with the dipole pointing perpendicular to the cell surfaces along the applied field. Due to the elastic nature of the director profile and smectic layering assumed in this model this would occur through most of the liquid crystal layer, with an increasingly wide region tending towards the extreme positions with increasing field strength. At large fields this would then lead to a large effective extinction angle between crossed polaroids for a conventional cell. The relaxed state (shown in figure 19 (*a*)) will, however, tend to have a guiding effect due to the slow variation of optic tensor twist angle across the cell, leading to a smaller extinction angle.

In the modelling here, it is assumed that the azimuthal angle varies smoothly and uniformly across the cell, and also that the layer tilt angle, δ (equal to the cone axis tilt angle) varies uniformly across the cell from θ to $-\theta$. Reflectivity curves are again calculated by dividing the cell into many layers to give a good model of the continuous nature of the ferroelectric liquid crystal layer. A theoretical reflectivity curve for R_{pp} with the cell in the parallel orientation for this model, with a cone angle θ of 24° is shown in figure 20. Again comparison of this model with the reflectivity data taken (figure 15) indicates that it does not adequately describe the optic tensor profile within the liquid crystal. The degree of s–p mixing is excessive in comparison with the data taken in the parallel cell orientation. In order for the magnitude of this to be reduced there needs to be less twist in the cell. (Tilt does not affect the s–p mixing in this orientation of the cell.) The question then arises as to how this may be accomplished. If

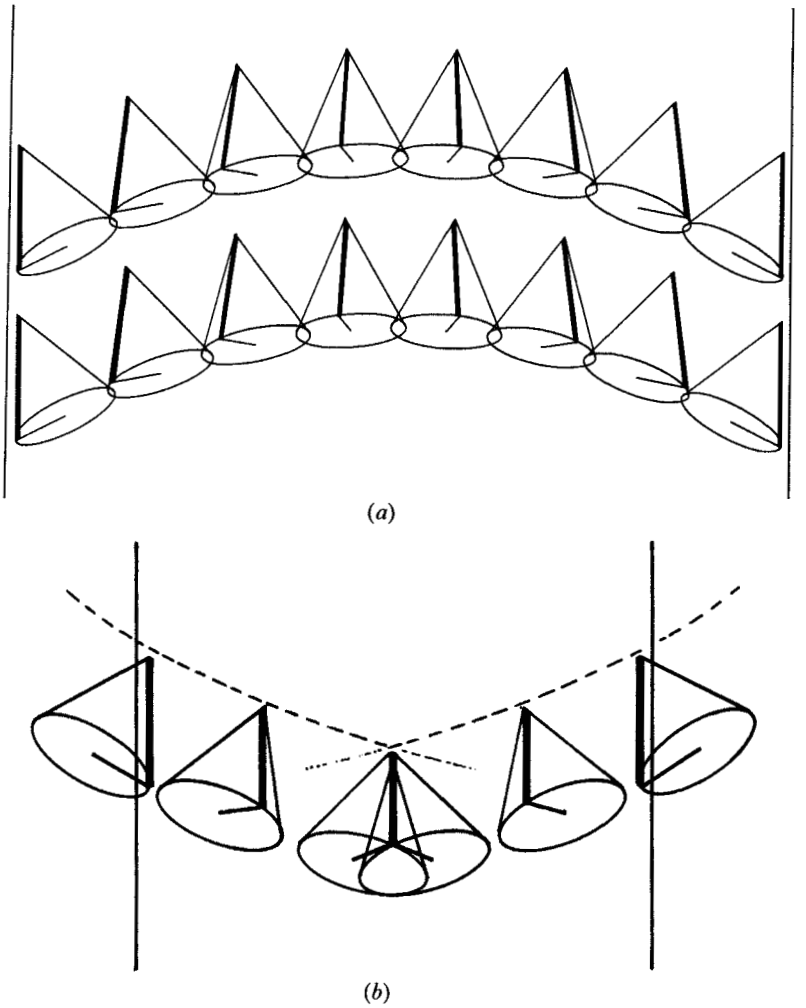

Figure 19. Schematic diagram of the banana model which has $\phi_0 = \pm 90°$ on the cell surfaces. (*a*) Allowing the smectic layers to bend uniformly across the cell, keeping the optic axis approximately parallel to the surfaces. (*b*) Including a kink in the middle of the sample to reduce the maximum optic tensor twist angle to less than the cone angle.

the smectic layering in the S_C^* phase distorts in some uniform way across the ferroelectric liquid crystal layer, then for a positive δ on one surface and a negative δ on the other, at some point between the surfaces in the cell $\delta = 0$. Then

$$\text{twist} = \arctan(\tan\theta\cos\phi),$$

$$\text{tilt} = \arcsin(\sin\theta\sin\phi),$$

where θ is the cone angle and ϕ is the azimuthal angle. This means that at this point either there is a high twist angle present or a high tilt angle or some combination of both. From the various models which have been considered thus far it seems that this is not a desirable situation.

One way to overcome this problem in the modelling is to allow a discontinuity in the smectic layer tilt angle at some point in the cell. If this occurred, then for the optic tensor profile (equivalent to the mechanical director) to be continuous across such a point, a discontinuity in the azimuthal angle ϕ would also occur. Then the optic tensor axis need not twist to the cone angle θ at this point. The continuity condition at such a point, assuming that the smectic layer tilt angle changes sign across it, would be given by

$$\tan \delta = \tan \theta \sin \phi.$$

Thus the azimuthal angle ϕ would also change sign across this point. The twist angle is then given by

$$\sin (\text{twist}) = \sin \theta \cos \phi.$$

In this situation a kinked banana model can be proposed as illustrated in figure 19 (*b*). The possible existence of this kinked banana model depends on a balance between the energy cost of the bending of the smectic layer tilt angle from $\delta = +\theta$ on one side of the cell to $\delta = -\theta$ on the other, and the energy cost of a kink in the smectic layer tilt angle in the middle of the cell. It is evident from the continuity at the point of the kink that the actual director profile is continuous across the cell, though if the director is mechanically biaxial the discontinuity in the azimuthal angle ϕ at the kink would cost energy. Possibly the energy cost of a kink plus a small bend is the lowest. In this model the smectic layer tilt δ in the middle of the cell and the continuity condition on the optic tensor introduces a twist angle of $\chi_0 = \arcsin (\sin \theta \cos \phi)$ in the middle of the cell, from the previous equation. Then across the cell the twist angle varies from 0° to χ_0 to 0°, rather then 0° to θ to 0°. The tilt again remains low throughout the cell in this model.

Attempting to fit the data with a model of this nature has shown that it is much more reasonable than those previously considered. Optimization of the twist angle χ_0 in the middle of the cell at the point of the kink, and also of the ferroelectric liquid

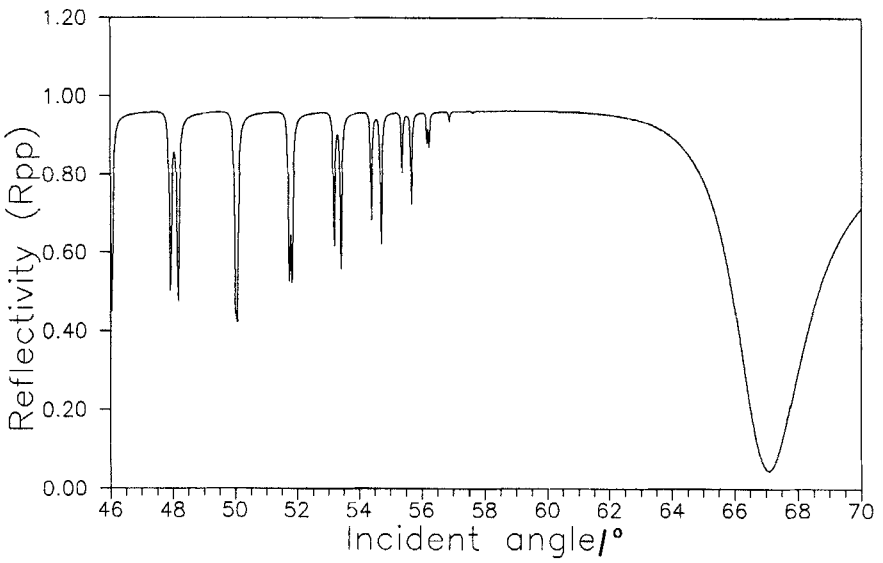

Figure 20. Theoretical reflectivity curve for the banana model with the cell in the parallel orientation.

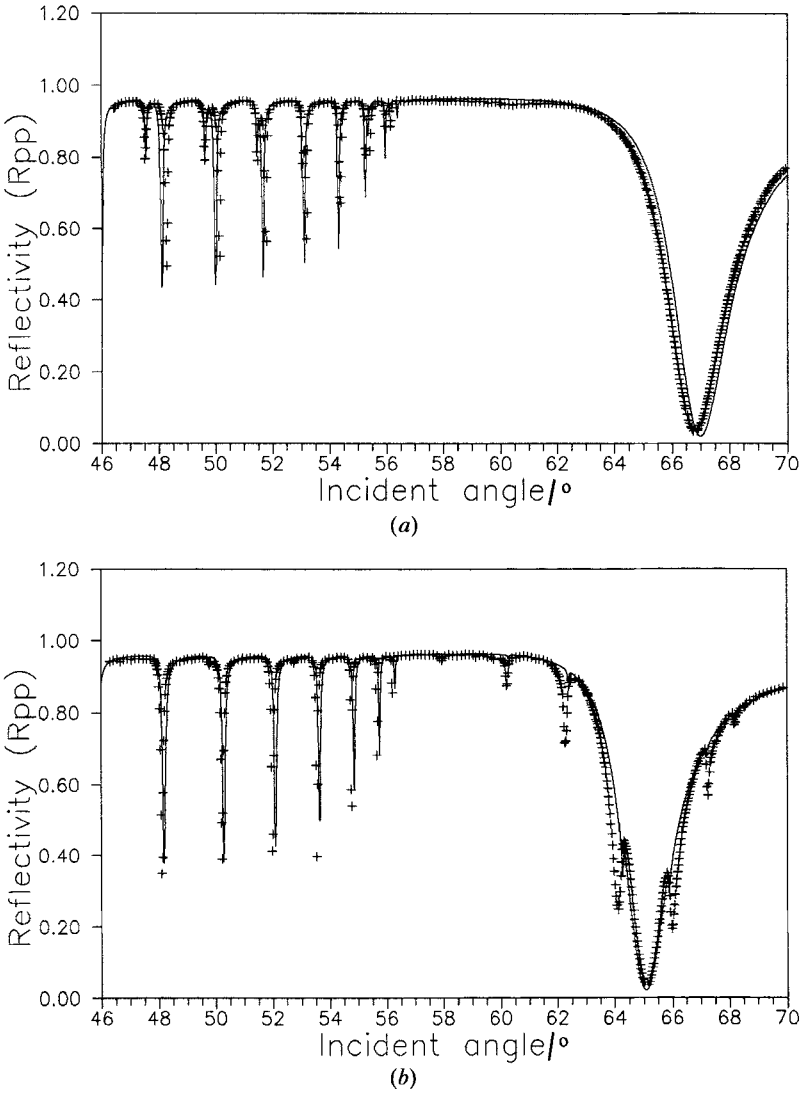

Figure 21. R_{pp} reflectivity theory (the line) and data (the crosses) for (*a*) parallel orientation and (*b*) perpendicular orientation of the cell. Kinked banana model with a maximum twist angle of about 12° in the middle of the cell.

crystal optic tensor dielectric constants results in a fit to the data shown in figure 21. Here the data are plotted as crosses on top of the theoretical continuous line, and we show fits for both orientations of the cell, as the discrepancies between theory and data are considerably smaller than before; this illustrates the quality of the fit well. Clearly this is a far more reasonable model than those tried previously, though errors in the mode positions are still evident.

But is this a sufficiently good model of the actual optic tensor configuration present or can it be improved? Initially the originally proposed bookshelf model retaining the perpendicular smectic layers of the S_A phase in the S_C^* phase was considered. The failure of this leads on to the consideration of the banana model and in order to reduce the

level of s–p mixing in the parallel cell orientation, the kinked-banana model. Now if the resulting fit from this in figure 21 (*a*) is examined carefully it is seen that for higher modes there is a considerable discrepancy between the position of the p-like modes, i.e. those most strongly excited by p-polarized light, in the theory and the data. This is because the sample thickness has been chosen to place the s-like modes in the correct positions, rather than the p-like ones. For these high order p-like modes the theoretical resonance occurs at too high an angle of incidence. It is more correct to note that the splitting between the p- and s-like modes is insufficient at these lower angles. Referring to the earlier modelling with larger twist angles it is seen that a larger twist angle increases the splitting in the high order modes. These higher order modes have E fields which extend nearer to the cell surfaces than the low order modes. (This can be seen in the E field distribution illustrations shown in figure 2.) So the requirement for a larger splitting between the p- and s-like modes at higher mode order indicates the requirement for a larger twist angle near the cell surfaces. This point is further indicated if the perpendicular cell orientation situation is considered. In this the level of s–p mixing through the surface plasmon-polariton resonance is rather weak in the theory compared with that present in the data (see figure 21 (*b*)). This indicates the need for a greater degree of twist in the optic tensor orientation within the surface plasmon-polariton penetration depth, i.e. near the cell surfaces. (It also shows the usefulness of the surface plasmon-polariton resonance.)

If the optic tensor is to stay relatively flat in the plane of the cell surfaces then for this to occur a greater amount of the smectic layers needs to be tilted. Taking this to the limit, the model for the ferroelectric liquid crystal layer in the cell becomes a uniform slab of dielectric material with the optic tensor twisted from the alignment axis by a constant angle χ. The smectic layers are then planar with a discontinuity of tilt angle in the middle of the cell; the layer tilt angle δ is

$$\delta = \arctan(\tan\theta \sin\phi).$$

This model with a planar discontinuity in the smectic layering at the centre of the cell is termed the chevron model [5]; such a situation is illustrated in figure 22. Modelling the liquid crystal layer in this way with a twist angle χ of 13° across the cell, and again optimizing the other parameters (still assuming uniaxiallity) leads to the fits for R_{pp} data shown in figure 23. The sample parameters found in this way are $\varepsilon_\perp = 2{\cdot}249 + 0{\cdot}001i$, $\varepsilon_\parallel = 2{\cdot}861 + 0{\cdot}001i$ with a cell thickness of 3·49 μm. The error bounds are as discussed earlier.

This new model gives a very good fit to the data, and is superior to the kinked banana model shown in figure 21. This chevron structure in the smectic layering has previously been observed in the S_C^* phase using X-ray scattering techniques by Pelzl [4] and Rieker [5]. The reason for its formation arises from the continuity of the smectic layers density wave when crossing a phase transition. The thickness of the smectic layers decreases on entering the S_C^* phase from the S_A phase, due to the biasing of the molecular axis away from the layer normal. The pitch in the smectic layering formed in the S_A phase is retained if the S_C^* phase is to form without disclinations. This leads to tilted smectic layers, with the tilt angle δ determined by

$$d_C = d_A \cos\delta,$$

where d_C is the smectic layer thickness in the S_C^* phase and d_A is the layer thickness in the S_A phase [5]. For this to be satisfied and the smectic layering to form in an unbroken

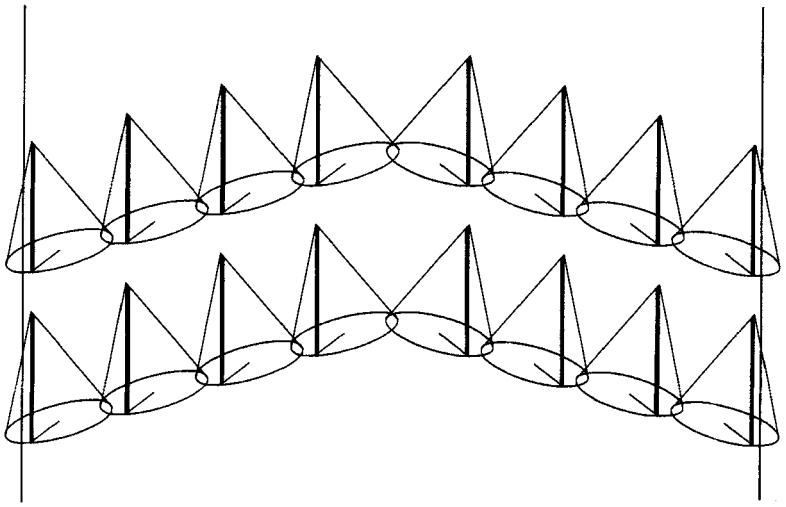

Figure 22. Schematic diagram of the chevron model which has a layer tilt of $\pm\delta$ and a smectic layer kink in the middle of the cell, leading to a constant optic tensor twist angle.

way in the S_C^* phase, the chevron structure in the layers forms and the optic tensor configuration is dictated by this. If the flat-in-the-plane condition is held at the surfaces then the result is the optically uniform layer of liquid crystal material used in the model here. Thus it seems that, as opposed to the bookshelf model, the development here has led to an optical confirmation of the chevron structure observed by X-ray scattering techniques. The analysis indicates that such a uniform twisted ferroelectric liquid crystal layer model (the kink in the middle of the cell being optically irrelevant) is a good description of the optic tensor configuration in a real cell. However it must now be checked that this result is within the bounds of experimental errors. In order to do this various perturbations will be made on the model and their effect on theoretical reflectivity curves noted.

The introduction of a small amount of biaxiality, such that $\varepsilon_2' \neq \varepsilon_3'$, represents a splitting in what is conventionally termed n_O, the ordinary refractive index. This is found not to improve the quality of the fit to the data using the chevron model. Addition of biaxiality representing a split in n_O of greater than about 0·001(5) ($|\varepsilon_2' - \varepsilon_3'| > 0{\cdot}004$) causes a noticeable perturbation on the resonant guided mode positions which is detrimental to the quality of fit with the data. Hence we conclude that if there is biaxiality present it is less than about 0·0015 in the refractive index n_O for SCE3. With SiO oblique (60° evaporation) alignment the surface tilt in the nematic phase is zero. However it could be that the elastic forces in the S_C^* phase introduce a bulk tilt of some kind. For example, the resistance to twist may cause a tilt in the bulk of the material in order to retain the chevron angle dictated by smectic layer density wave matching between phases. Introduction of such tilt does not improve the theoretical fit to the data and indicates that the bulk tilt is less than approximately 2°. Tilts below this are insufficient to be observed using this method, though small surface tilts increase the level of s–p mixing through surface plasmon-polariton in the perpendicular orientation. It is feasible that in the chevron structure there exists some boundary layer regions at the chevron interface (where the smectic layer tilt angle reverses) and/or adjacent to the cell surfaces. The problem with any such idea is that it is very difficult to

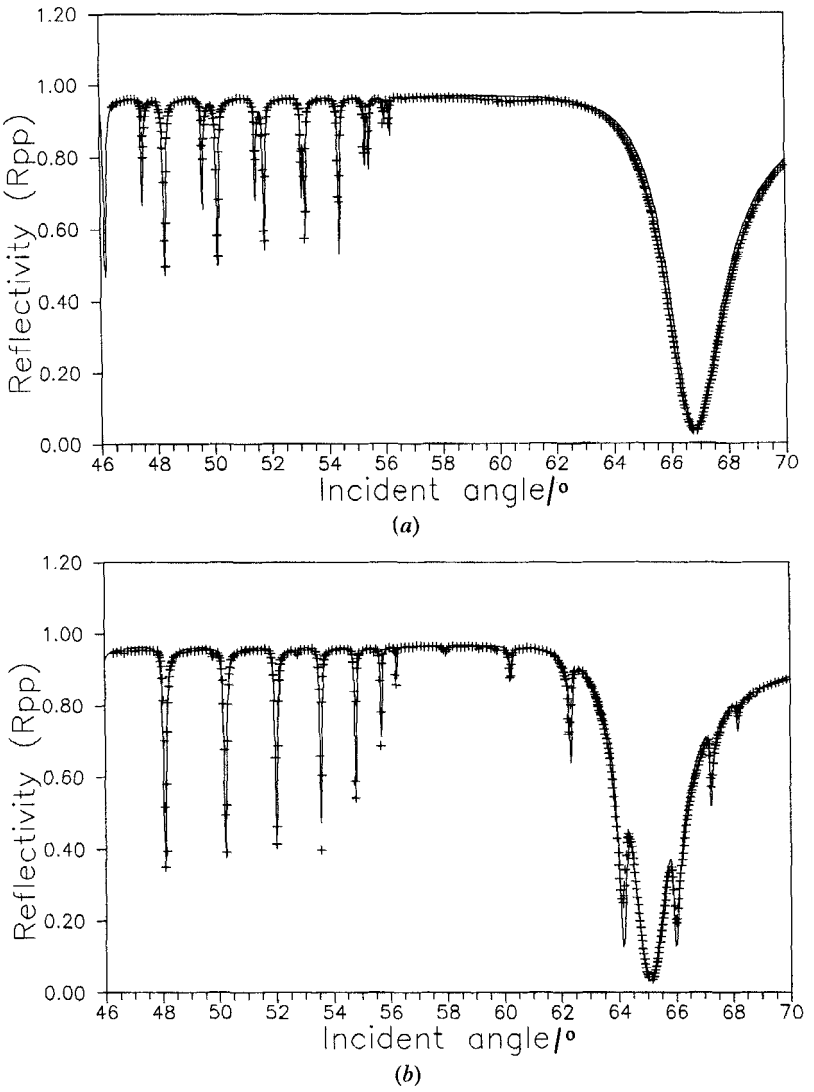

Figure 23. R_{pp} reflective theory (the line) and data (the crosses) for (*a*) parallel orientation and (*b*) perpendicular orientation of the cell. Chevron model, with the ferroelectric liquid crystal layer equivalent to a uniform slab of material twisted from the surface alignment direction.

know the structure of such regions, and difficult, therefore, to model them. If such a region exists at the chevron interface, what might its form be? It could be that the chevron interface is a very rapid kink [22]. Including such a region in the middle of the ferroelectric liquid crystal layer perturbs some of the resonant modes and reduces the quality of the theoretical fit to the data if it is > 100 nm thick. This indicates that if such a region exists it must be < 100 nm thick. This is not such a precise constraint as that placed upon the chevron kink by X-ray scattering work, which implies a region of thickness $< \sim 100$ Å [22]. There is also the possibility of a boundary layer region at the cell surfaces. This could take the form of a rapid reorganization from the bulk optic

tensor alignment to the surface alignment direction. It is, perhaps, unlikely that the mechanical director actually twists from the surface alignment direction right at the surface. The bulk twist angle dictated by the smectic layering chevron structure would not then extend to the surface, but to within some small distance over which the structure would reorganize. Xue *et al.* have observed that, with no surface treatment, any unswitched region (equivalent here to any boundary layer region) must be less than 2 nm thick [23]. This is to be expected since with no surface treatment the only restriction is that the mechanical director tends to lie in the plane of the surface. However, here the director tends to lie in the surface alignment direction and a thin layer of reorganization can feasibly exist. Including this in the modelling as a variation between the surface alignment direction ($\chi = 0$) and the bulk twist angle ($\chi \approx 13°$) over a finite region indicates that it is not greater than the order of 100 nm thick. Introduction of such regions does not significantly affect the positioning of the guided modes, since their field intensity drops to zero at the silver surfaces anyway. Regions thicker than this do though have an effect on the surface plasmon-polariton resonance position which has a finite component of electric field perpendicular to the cell surfaces, though due to the zero (or near zero) level of the tangential field the dependence on twist angle is weak.

It seems, therefore, that if any regions do exist at the chevron interface or cell surfaces which are not aligned with the bulk of the ferroelectric liquid crystal in the cell that they are thin, being less than or of order 100 nm. This, therefore, represents a limit on the accuracy of the result from this work that the liquid crystal layer is equivalent to a uniform slab of material twisted from the surface alignment direction.

5. Comparison with conventional cells

The conclusion of the work here on SCE3 is that the ferroelectric liquid crystal layer is in the main equivalent to an optically uniform slab of dielectric material twisted by a few degrees from the surface alignment direction. This is consistent with the chevron structure in the smectic layering of the S_C^* phase [5]. SCE3 is found to be uniaxial within experimental errors. However, in a conventional cell observed between crossed polaroids this would lead to a perfect extinction when the optic tensor major axis is aligned parallel to either the polarizer or the analyser direction. Then the incident light would remain plane polarized travelling through the ferroelectric liquid crystal layer and no transmission through the analyser would result for any incident wavelength. This, however, is not the case in a real cell. It is normally observed that the extinction between crossed polaroids is not perfect, and there is no cell orientation which extinguishes all incident wavelengths [24]. Figure 24 shows transmission as a function of incident wavelength taken between crossed polaroids for a conventional cell with low tilt SiO surface alignment. The transmission at what would normally be termed extinction ($+10°$) rises at low wavelengths. If the optically uniform slab model was totally correct this would not be so and a perfect extinction angle would exist. How can this be reconciled with the results presented here? It was seen that thin boundary layers adjacent to the cell surfaces of $\sim 0{\cdot}1\ \mu$m (100 nm) could be present but could neither be confirmed nor repudiated by fitting the guided mode data, for if they existed they would not significantly affect the results of this work. Now it is known from nematic work that if

$$P \gg \frac{\lambda}{\Delta n},$$

where P is the pitch of twist variation in a sample, λ is the wavelength of light and Δn is the optical anisotropy then the plane of polarization of the light follows the twist, and guiding of the plane of polarization occurs (the Mauguin limit). But if

$$P \ll \frac{\lambda}{\Delta n},$$

then the plane of light polarisation is not changed when it propagates through a sample. However if

$$P \sim \frac{\lambda}{\Delta n},$$

then a critical condition occurs, and the light may not remain plane polarized in a sample. Here

$$\frac{\lambda}{\Delta n} \sim 3{\cdot}5\ \mu\text{m},$$

thus a twist from 0° to about 10° over $\sim 0{\cdot}1\ \mu$m satisfies the critical condition. Thus it seems that a boundary layer region of twist variation from the surface alignment direction to the bulk twist angle over a thickness of $\sim 0{\cdot}1\ \mu$m could possibly explain the lack of extinction in a real cell, and be consistent with the observations made here that the ferroelectric liquid crystal layer is largely optically equivalent to a uniform slab of dielectric material. Such boundary layer regions have been noted before in s–p mixing studies of polymer aligned devices [25].

It has been shown by Anderson *et al.* [24] that a useful way to analyse spectroscopic transmission studies of liquid crystal cells is to plot the extinction angle as a function of wavelength. This removes any normalization difficulties in plotting the actual

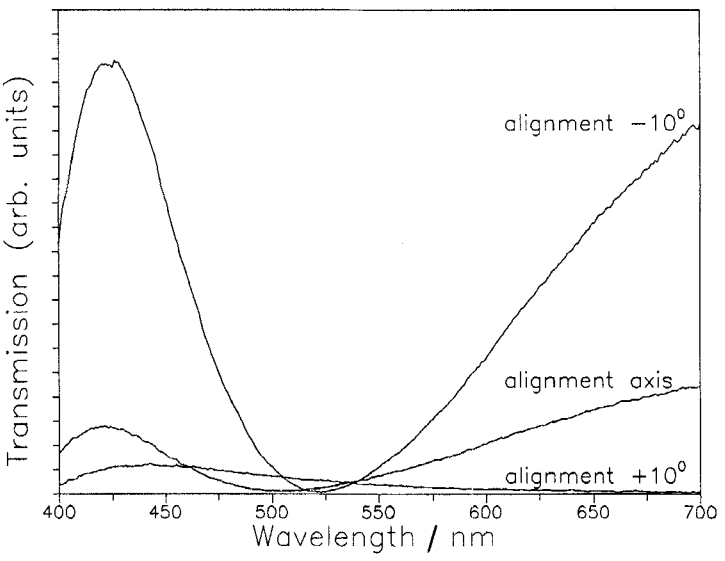

Figure 24. Transmission against wavelength data for a SCE3 filled cell between crossed polaroids (cell $\sim 2{\cdot}7\ \mu$m thick).

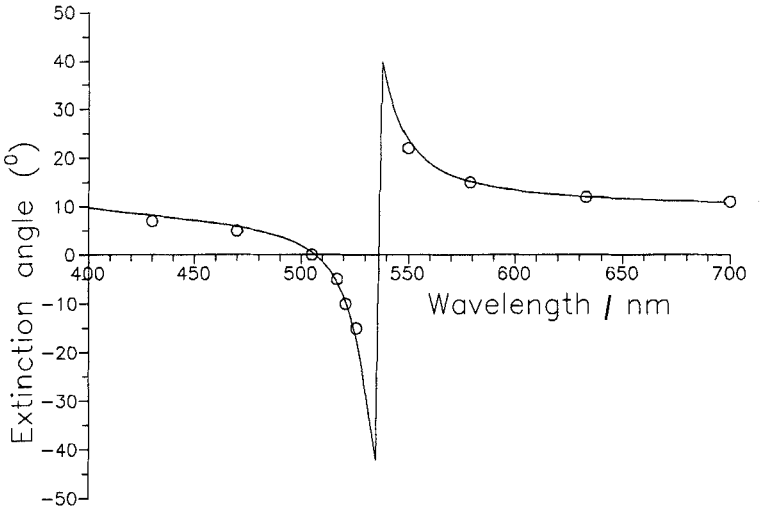

Figure 25. Fit to extinction angle as a function of wavelength extracted from the transmission data. Theory obtained for a uniform model with boundary layers of $\sim 0{\cdot}2\,\mu$m thickness. (The data are the circles, theory is the continuous line.)

transmission data. Modelling a cell with boundary layer regions of varying twist angle and plotting extinction angle against wavelength leads to the fit shown in figure 25. Here dispersion of Δn with wavelength has been allowed for, and in this cell boundary layer regions of $\sim 0{\cdot}2\,\mu$m thickness were required. This is a little greater than anticipated, but the dominant E field component in the surface localized surface plasmon-polariton resonance is normal to the cell surface, and thus variation in the optic tensor twist angle near the surface of the cell has only a small effect.

It seems, therefore, that this is a reasonable explanation of both the data in this work and the transmission data for a conventional cell. The thin boundary layers are of sufficient thickness to cause a failure of extinction in a real cell, but insufficient to significantly affect the guided modes and surface plasmon-polariton resonance in this work. The precise physical nature of the boundary layer regions in quite difficult to ascertain, but may involve a breakdown in the general structure of the smectic layering over a thin ($\sim 0{\cdot}1$–$0{\cdot}2\,\mu$m) region of reorganization from bulk alignment dictated by the smectic layers and surface alignment direction held from the higher temperature phases. Variation of this boundary region over the surface of a cell may explain the texture often seen within monodomains in real cells.

6. Summary

In this paper we have discussed the configuration in a ferroelectric liquid crystal cell filled with BDH material SCE3, in the relaxed state, i.e. no field applied. In conclusion we have seen that the ferroelectric liquid crystal layer is largely optically equivalent to a uniform slab of dielectric material which is twisted from the surface alignment direction by a few degrees. This eliminates the possibility of models such as the bookshelf model where the smectic layering stays perpendicular to the cell surfaces in the S_C^* phase. The reason for the observed optic tensor orientation is the domination of the smectic layering in the formation of the structure in a cell. The layer shrinkage in the S_C^* phase leads to a chevron structure in the layering and the optic tensor is forced to take on a

configuration which is consistent with this. In the case here, with planar SiO boundary conditions this results in an optically, largely uniform slab, thus providing direct optical confirmation of the chevron structure in such cells. For a tilted surface condition the alignment resulting can be different [24, 25]. This result is for SCE3, and while other materials may take on differing configurations due to different elasticity and surface alignment conditions the structures formed in each case should be consistent with the chevron structure in the smectic layering. For example the boundary layer region introduced to explain the effects seen in conventional cells may vary with variation of material parameters.

Optical work of this type provides a powerful method for the examination of the optic tensor configuration in a liquid crystal cell. It is the only way in which both the twist and tilt of optic tensor orientation can be observed, and is a very useful tool in the determination of ferroelectric liquid crystal cell parameters.

The author thanks J. R. Sambles of Exeter University and M. G. Clark of GEC Research Ltd., Wembley, for supervision, help and encouragement. Also the financial support of the SERC and the Wolfson trust is acknowledged.

References

[1] MEYER, R. B., LIEBERT, L., STRZELECKI, L., and KELLER, P., 1975, *J. Phys., Lett., Paris*, **36,** L69.
[2] CLARK, N. A., and LAGERWALL, S. T., 1980, *Appl. Phys. Lett.*, **36,** 899.
[3] OUCHI, Y., TAKANO, H., TAKEZOE, H., and FUKUDA, A., 1987, *Jap. J. appl. Phys.*, **26,** L21.
[4] PELZL, G., KOLBE, P., PREUKSCHAS, V., DIELE, S., and DEMUS, D., 1979, *Molec. Crystals liq. Crystals*, **53,** 167.
[5] RIEKER, T. P., CLARK, N. A., SMITH, G. S., PARMAR, D. S., SIROTA, E. B., and SAFINYA, C. R., 1987, *Phys. Rev. Lett.*, **59,** 2658.
[6] WELFORD, K. R., SAMBLES, J. R., and CLARK, M. G., 1987, *Liquid Crystals*, **2,** 91.
[7] ELSTON, S. J., SAMBLES, J. R., and CLARK, M. G., 1989, *J. Mod. Opt.*, **36,** 1019.
[8] TIEN, P. K., 1971, *Appl. Optics*, **10,** 2395.
[9] TIEN, P. K., 1977, *Rev. mod. Phys.*, **49,** 361.
[10] WELFORD, K. R., 1986, Thesis, Exeter, England.
[11] AZZAM, R. M. A., and BASHARA, N. M., 1979, *Ellipsometry and Polarised Light* (North-Holland).
[12] IOP Short Meetings Series No. 9, 1988, *Surface Plasmon Polaritons*, edited by R. A. Innes and K. R. Welford.
[13] WELFORD, K. R., and SAMBLES, J. R., 1987, *Appl. Phys. Lett.*, **50,** 871.
[14] HORNAUER, D., and RAETHER, H., 1973, *Optic. Commun.*, **7,** 297.
[15] BARNES, W. L., 1986, Thesis, Exeter, England.
[16] BERREMAN, D. W., and SCHEFFER, T. J., 1970, *Phys. Rev. Lett.*, **25,** 577.
[17] KO, D. Y. K., and SAMBLES, J. R., 1988, *J. opt. Soc. Am. A*, **5,** 1863.
[18] INNES, R. A., 1987, Thesis, Exeter, England.
[19] TAKEZOE, H., OUCHI, Y., ISHIKAWA, K., and FUKUDA, A., 1986, *Molec. Crystals liq. Crystals*, **139,** 27.
[20] CLARK, M. G., BOWRY, C., MOSLEY, A., and NICHOLAS, B. M., 1987, *Proceedings of FLC87, Ferroelectrics*, **84, 85.**
[21] KONDO, K., TAKEZOE, H., FUKUDA, A., KUZE, E., FLATISCHLER, K., and SKARP, K., 1983, *Jap. J. appl. Phys.*, **22,** L294.
[22] CLARK, N. A., and RIEKER, T. P., 1988, *Phys. Rev.* A, **37,** 1053.
[23] XUE, J., CLARK, N. A., and MEADOWS, M. R., 1988, *Appl. Phys. Lett.*, **53,** 2397.
[24] ANDERSON, M. H., JONES, J. C., RAYNES, E. P., and TOWLER, M. J., 1991, *J. Phys.* D (in the press).
[25] LAVERS, C. R., and SAMBLES, J. R., 1990, *Liq. Crystals*, **8,** 577.